(1)

OFFICE OF NAVAL RESEARCH

CONTRACT N00014-89-J-1828

R&T Code 3132080

Abstract Report #1

CHIRAL RECOGNITION IN MOLECULAR AND MACROMOLECULAR PAIRS OF LIQUID CRYSTALS OF (2R, 3S)- AND (2S, 3S)-2-FLUORO-3-METHYLPENTYL 4'-(11-VINYLOXYUNDECANYLOXY)BIPHENYL-4-CARBOXYLATE DIASTEREOMERS

by

V. Percec, H. Oda, P. L. Rinaldi and D. R. Hensley

Published

in the

Macromolecules, 27, 12 (1994)

Department of Macromolecular Science
Case Western Reserve University
Cleveland, OH 44106-7202

June 30, 1994

REPORT DOCUMENTATION PAGE

Form Approved
OMB No. 0704-0188

1. AGENCY USE ONLY (Leave blank)	2. REPORT DATE	3. REPORT TYPE AND DATES COVERED
	June 30, 1994	Abstract Report #1

4. TITLE AND SUBTITLE
Chiral Recognition in Molecular and Macromolecular Pairs of Liquid Crystals of (2R, 3S)- and (2S, 3S)-2-Fluoro-3-methylpentyl 4'-(...

5. FUNDING NUMBERS
N00014-89-J-1828

6. AUTHOR(S)
V. Percec, H. Oda, P. L. Rinaldi and D. R. Hensley

7. PERFORMING ORGANIZATION NAME(S) AND ADDRESS(ES)
Department of Macromolecular Science
Case Western Reserve University
Cleveland, OH 44106-7202

8. PERFORMING ORGANIZATION REPORT NUMBER
N00014-89-J-1828

9. SPONSORING/MONITORING AGENCY NAME(S) AND ADDRESS(ES)
Department of Navy
Office of Naval Research
800 North Quincy Street
Arlington, VA 22217-5000

10. SPONSORING/MONITORING AGENCY REPORT NUMBER
Abstract Report #1

11. SUPPLEMENTARY NOTES
Macromolecules, 27, 12 (1994)

12a. DISTRIBUTION/AVAILABILITY STATEMENT

12b. DISTRIBUTION CODE

13. ABSTRACT *(Maximum 200 words)*

(2R, 3S)-2-Fluoro-3-methylpentyl 4'-(11-vinyloxyundecanyloxy)biphenyl-4-carboxylate (**15**) (2R 92%ee) and (2S, 3S)-2-fluoro-3-methylpentyl 4'-(11-vinyloxyundecanyloxy)biphenyl-4-carboxylate (**16**) (2S 92%ee) diastereomers and their corresponding homopolymers and copolymers with well defined molecular weight and narrow molecular weight distribution were synthesized and characterized. The phase behaviors of **15** and poly(**15**) are identical to those of **16** and poly(**16**) respectively. The phase behavior of the two diastereomeric polymers can be compared *only* by superimposing the dependence of their transition temperatures as a function of molecular weight. Both monomers display enantiotropic S_A, monotropic S_C^* and crystalline phases, while the corresponding polymers exhibit enantiotropic S_A, S_C^* and S_X (unidentified smectic) mesophases. The phase behavior of the binary mixtures of **15** and **16** and poly(**15**) with poly(**16**) shows that they are miscible and therefore isomorphic within all their mesophases and over the entire range of compositions. This is in contrast to the crystalline phases of the monomers whose phase diagram displays an eutectic. The investigation of the binary copolymers poly(**15**-*co*-**16**) shows that the structural units derived from the two diastereomeric monomers are isomorphic within their enantiotropic S_A, S_C^* and S_X mesophases. The phase behavior of all these binary monomeric, polymeric and copolymeric systems shows that they form ideal solutions within all their mesophases and therefore, demonstrated the absence of chiral molecular recognition between the 2R and 2S stereogenic centers. Since the physical properties of diastereomers are most frequently different, these results are of unusual interest.

14. SUBJECT TERMS	15. NUMBER OF PAGES
	16. PRICE CODE

17. SECURITY CLASSIFICATION OF REPORT	18. SECURITY CLASSIFICATION OF THIS PAGE	19. SECURITY CLASSIFICATION OF ABSTRACT	20. LIMITATION OF ABSTRACT
unclassified	unclassified	unclassified	UL

Chiral Recognition in Molecular and Macromolecular Pairs of Liquid Crystals of (2R, 3S)- and (2S, 3S)-2-Fluoro-3-methylpentyl 4'-(11-Vinyloxyundecanyloxy)biphenyl-4-carboxylate Diastereomers

V. Percec* and H. Oda
Department of Macromolecular Science
Case Western Reserve University
Cleveland, OH 44106

P. L. Rinaldi and D. R. Hensley
Department of Chemistry
University of Akron
Akron, OH 44325

* To whom all correspondence should be addressed

Abstract

(2R, 3S)-2-Fluoro-3-methylpentyl 4'-(11-vinyloxyundecanyloxy)biphenyl-4-carboxylate (**15**) (2R 92%ee) and (2S, 3S)-2-fluoro-3-methylpentyl 4'-(11-vinyloxyundecanyloxy)biphenyl-4-carboxylate (**16**) (2S 96%ee) diastereomers and their corresponding homopolymers and copolymers with well defined molecular weight and narrow molecular weight distribution were synthesized and characterized. The phase behaviors of **15** and poly(**15**) are identical to those of **16** and poly(**16**) respectively. The phase behavior of the two diastereomeric polymers can be compared *only* by superimposing the dependence of their thermal transition temperatures as a function of molecular weight. Both monomers display enantiotropic S_A, monotropic S_C^* and crystalline phases, while the corresponding polymers exhibit enantiotropic S_A, S_C^* and S_X (unidentified smectic) mesophases. The phase behavior of the binary mixtures of **15** with **16** and poly(**15**) with poly(**16**) shows that they are miscible and therefore isomorphic within all their mesophases and over the entire range of compositions. This is in contrast to the crystalline phases of the monomers whose phase diagram displays an eutectic. The investigation of the binary copolymers poly(**15**-*co*-**16**) shows that the structural units derived from the two diastereomeric monomers are isomorphic within their enantiotropic S_A, S_C^* and S_X mesophases. The phase behavior of all these binary monomeric, polymeric, and copolymeric systems shows that they form ideal solutions within all their mesophases and therefore, demonstrates the absence of chiral molecular recognition between the 2R and 2S stereogenic centers. Since the physical properties of diastereomers are most frequently different, these results are of unusual interest.

Introduction

Stereochemistry is the most sensitive tool for probing the structural details on how molecules "see" each other as they come together to form crystals and transition states. Therefore, it represents the most powerful tool available in chemistry for the study and manipulation of molecular shapes and symmetry properties.[1] The most notable series of studies in this field refers to the investigation of chiral molecular recognition in monolayers of pure enantiomers and their pairs as well as in monolayers of pure diastereomers and their mixtures.[1a] Enantiomers are considered to be perfect physical and chemical models for each other since their properties, with the exception of the rotation of polarized light and those that involve their interactions with other chiral systems, are identical. Chiral discrimination between the properties of monolayers formed by pure enantiomers and their mixtures was always observed,[1,2] with the notable exception of phosphatidylcholines.[3]

In the field of molecular thermotropic liquid crystals, there are only few examples in which the phase diagrams of binary mixtures of enantiomeric compounds were investigated.[1c, 4, 5] *Only in three of these cases[4a, c, d] it has been observed that chiral molecular recognition occurs and it increases the phase transition temperatures of the 1/1 molar mixture by comparison to the one of the pure enantiomers.*

There are much fewer systems in which attempts were made to detect stereochemical recognition between pairs of diastereomers in monolayers. The first systematic study of the monolayer properties of a diastereomeric series was reported in 1988.[6a] By contrast to pairs of enantiomers[1a, 2] none of the first eight pairs of diastereomeric surfactants investigated showed stereoselectivity at the air-water interface.[6a] Only very recently the first example of chiral molecular recognition in monolayers of diastereomeric compounds was reported.[6b]

The first goal of this paper is to describe the synthesis and the living cationic polymerization of (2R, 3S)-2-fluoro-3-methylpentyl 4'-(11-vinyloxyundecanyloxy)biphenyl-4-carboxylate (**15**) and (2S, 3S)-2-fluoro-3-methylpentyl 4'-(11-vinyloxyundecanyloxy)-biphenyl-4-carboxylate (**16**) diastereomers. The second goal of this paper is to compare the mesomorphic behavior of these two diastereomeric structural units and to investigate their isomorphism in binary monomer and polymer mixtures, and in binary copolymers. To our knowledge, this paper reports the first investigation on the chiral molecular recognition of molecular and macromolecular pairs of diastereomeric liquid crystals.

Experimental Section

Materials

L-Isoleucine [(2S,3S)-(+)-2-amino-3-methylpentanoic acid, 99%], tetrabutylammonium fluoride hydrate (n-$Bu_4NF{\cdot}xH_2O$, 98%), tetrabutylammonium hydrogen sulfate (TBAH, 98%) and pyridinium poly(hydrogen fluoride) (HF 70% by weight) (all from Aldrich) were used as received.

$NaNO_2$ (Fisher) was dried at 140°C under vacuum for 40 hours before each use. Trifluoromethanesulfonic anhydride was prepared from CF_3SO_3H (Lancaster, 98+%) and P_2O_5 according to a literature procedure.[7a, b]

Pyridine was heated overnight at 100°C over KOH, distilled from KOH, and then stored over KOH. CH_2Cl_2 was refluxed over CaH_2 overnight and distilled from CaH_2. Dimethyl sulfoxide (DMSO) was heated overnight at 100°C over CaH_2, distilled from CaH_2 under vacuum, and stored over molecular sieves 4Å. Tetrahydrofuran (THF) was first distilled from $LiAlH_4$ and further dried over Na/benzophenone.

CH_2Cl_2 used as polymerization solvent was first washed with concentrated H_2SO_4 several times until the acid layer remained colorless, then washed with water, dried over

$MgSO_4$, refluxed over CaH_2, and freshly distilled under argon before each use. $S(CH_3)_2$ used in polymerizations (Aldrich, anhydrous, 99+%, packed under nitrogen in Sure/Seal™ bottle) was used as received. CF_3SO_3H used as a polymerization initiator (Aldrich, 98%) was distilled under vacuum.

All other materials were commercially available and were used as received.

Techniques

^{1}H-NMR (200MHz) spectra were recorded on a Varian XL-200 spectrometer. ^{19}F decoupled ^{1}H-NMR (300MHz) spectra and ^{19}F-NMR spectra were recorded on a Varian VXR-300 spectrometer. In order to determine the chemical shifts of ^{19}F resonances a ^{19}F spectrum of $CF_3C_6H_5$ was first acquired since its ^{19}F resonance is known from literature[8] to appear at 63.72ppm (referenced against $CFCl_3$ at 0.00ppm). Then sample spectra were acquired using the identical parameters.

Relative molecular weights of polymers were determined by gel permeation chromatography (GPC). GPC analyses were carried out with a Perkin-Elmer Series 10LC instrument equipped with an LC-100 column oven and a Nelson Analytical 900 Series data station. Measurements were made by using a UV detector, THF as solvent (1ml/min, 40°C), a set of PL gel columns of $5x10^2$ and 10^4Å, and a calibration plot constructed with polystyrene standards. High pressure liquid chromatography (HPLC) experiments were performed with the same instrument.

A Perkin-Elmer DSC-4 differential scanning calorimeter equipped with a TADS 3600 data station was used to determine the thermal transition temperatures, which were reported as the maxima and minima of their endothermic or exothermic peaks respectively. In all cases heating and cooling rates were 20°C/min.

A Carl-Zeiss optical polarizing microscope equipped with a Mettler FP-82 hot stage and a Metter FP-80 central processor was used to observe the thermal transitions and to analyze the anisotropic textures.

Synthesis of monomers

Monomers **15** and **16** were synthesized according to Scheme 1. The synthesis of compounds **11** and **14** was described previously.[9]

(2S, 3S)-2-Hydroxy-3-Methylpentanoic Acid (2)[10]

A solution of $NaNO_2$ (39.4g, 0.572mol) in water (150ml) was added dropwise to a stirred, cooled (0°C) mixture of L-isoleucine (49.5g, 0.377mol), concentrated H_2SO_4 (16ml) and water (570ml). The mixture was allowed to warm to room temperature and stirred

overnight. The product was extracted into diethyl ether three times and the combined ethereal extracts were dried over anhydrous $MgSO_4$. The crude product (39.5g) obtaind after the evaporation of the solvent was used for the synthsis of compound 3 without further purification. ^{1}H-NMR (DMSO-d_6, TMS, δ, ppm): 0.84 (t, J=7.2Hz, 3H, $C\underline{H}_3CH_2$-), 0.87 (d, J=6.4Hz, 3H, -CH ($C\underline{H}_3$)-), 1.02-1.29, 1.29-1 53 (m, 2H, $CH_3C\underline{H}_2$-), 1.53-1.57 (m, 1H, -$C\underline{H}(CH_3)$-), 3.79 (d, J=4.8Hz, 1H, -$C\underline{H}$(OH)-).

Ethyl (2S, 3S)-2-Hydroxy-3-Methylpentanoate (3)[10a]

A stirred mixture of 2 (crude 39.5g), anhydrous ethanol (300ml) and concentrated H_2SO_4 (7.5ml) was heated under reflux overnight. Ethanol was distilled off and the residue was diluted with diethyl ether. This ether solution was washed with saturated $NaHCO_3$ solution twice and dried over anhydrous $MgSO_4$. Ether was evaporated off and the remained crude product was distilled under vacuum to yield a colorless liquid (34.5g, 57.1% from L-isoleucine); bp 62-65°C at 6mmHg. ^{1}H-NMR ($CDCl_3$, TMS, δ, ppm): 0.91 (t, J=7.4Hz, 3H, $C\underline{H}_3CH_2CH(CH_3)$-), 0.99 (d, J=6.7Hz, 3H, -CH($C\underline{H}_3$)-), 1.13-1.53 (m, 2H, $CH_3C\underline{H}_2$-$CH(CH_3)$-), 1.31 (t, J=7.1Hz, -$COOCH_2C\underline{H}_3$), 1.73-1.93 (m, 1H, -$C\underline{H}(CH_3)$-), 2.78 (bs, 1H, -CH(O$\underline{H}$)-), 4.08 (d, J=3.6Hz, 1H, -$C\underline{H}$(OH)-), 4.26 (dq, J=7.1, 1.7Hz, 2H, -$COOC\underline{H}_2CH_3$).

Ethyl (2S, 3S)-2-Trifluoromethanesulfonyloxy-3-Methylpentanoate (4)[7, 10a]

Freshly prepared trifluoromethanesulfonic anhydride (50.0g, 0.177mol) was added dropwise to a stirred, cooled (0°C) solution of 3 (23.8g, 0.149mol) in dry CH_2Cl_2 (200ml) and pyridine (18.6ml, 0.230mol) under nitrogen atmosphere. The mixture was allowed to warm to room temperature and stirred for 2 hours. Then the mixture was poured into water and the product was extracted into CH_2Cl_2 twice. The combined organic layers were washed with 10% HCl twice and dried over anhydrous $MgSO_4$. The solvent was evaporated off and the remained crude product was distilled under vacuum to yield a colorless liquid (37.2g, 85.4%); bp 55-61°C at 0.4mmHg. ^{1}H-NMR ($CDCl_3$, TMS, δ, ppm): 0.95 (t, J=7.4Hz, 3H, $C\underline{H}_3CH_2CH(CH_3)$-), 1.07 (d, J=7.0Hz, 3H, -CH($C\underline{H}_3$)-), 1.19-1.64 (m, 2H, $CH_3C\underline{H}_2CH(CH_3)$-), 1.33 (t, J=7.2Hz, 3H, -$COOCH_2C\underline{H}_3$), 2.05-2.27 (m, 1H, -$C\underline{H}(CH_3)$-), 4.31 (dq, J=7.2, 1.9Hz, 2H, -$COOC\underline{H}_2CH_3$), 5.01 (d, J=3.9Hz, 1H, -$C\underline{H}(OSO_2CF_3)$-).

Ethyl (2R, 3S)-2-Fluoro-3-Methylpentanoate (5)[10a]

A solution of 4 (36.7g, 0.126mol) in acetonitrile (50ml) was added dropwise to a stirred, cooled (0°C) solution of terabutylammonium fluoride hydrate (n-$Bu_4NF{\cdot}xH_2O$, 40g) in acetonitrile (150ml). The stirred mixture was heated under reflux for 3 hours. Then acetonitrile was evaporated off and the remained mixture was passed through a silica gel

short column using hexane-ethyl acetate (10:1) as an eluent. The solvent was evaporated off and the crude product was distilled under vacuum to yield a colorless liquid (16.7g, 81.9%); bp 59-63°C at 9mmHg. ^{1}H-NMR ($CDCl_3$,TMS, δ, ppm): 0.95 (d, J=6.5Hz, 3H, -CH($C\underline{H}_3$)-), 0.96 (t, J=8.3Hz, 3H, $C\underline{H}_3CH_2CH(CH_3)$-), 1.19-1.65 (m, 2H, $CH_3C\underline{H}_2CH(CH_3)$-), 1.32 (t, J=7.0Hz, 3H, -$COOCH_2C\underline{H}_3$), 1.75-2.12 (m, 1H, -C$\underline{H}$(CH_3)-), 4.28 (q, J=7.0Hz, 2H, -$COOC\underline{H}_2CH_3$), 4.86 (dd, J=48.5, 3.1Hz, 1H, -C$\underline{H}$F-).

(2R, 3S)-2-Fluoro-3-Methylpentanol (6)[10a]

A solution of **5** (16.4g, 0.101mol) in dry THF (100ml) was added dropwise to a stirred, cooled (-70°C) mixture of $LiAlH_4$ (5.69g, 0.150mol) and dry THF (100ml) under nitrogen atmosphere. The stirred mixture was allowed to warm to room temperature and then heated under reflux for 2 hours. Excess $LiAlH_4$ was quenched with ethyl acetate (50ml) and the mixture was treated with 10% HCl (300ml). The product was extracted into ethyl acetate twice and the combined organic layers were dried over anhydrous $MgSO_4$. The solvent was evaporated off and the remained crude product was purified by column chromatography (silica gel; hexane-ethyl acetate 10:1 and 5:1) to give a colorless liquid (8.51g, 70.1%). ^{1}H-NMR ($CDCl_3$, TMS, δ, ppm): 0.93 (t, J=7.6Hz, 3H, $C\underline{H}_3CH_2$-), 0.95 (d, J=7.0Hz, 3H, -CH-($C\underline{H}_3$)-), 1.08-1.29, 1.36-1.76 (m, 3H, $CH_3C\underline{H}_2C\underline{H}(CH_3)$-), 2.81 (bs, 1H, -O$\underline{H}$), 3.56-3.92 (m, 2H, -$C\underline{H}_2$OH), 4.25-4.39, 4.50-4.62 (m, 1H, -C$\underline{H}$F-).

(2R, 3S)-2-Fluoro-3-Methylpentyl Tosylate (7)

A solution of **6** (4.0g, 33.3mmol) in dry pyridine (15ml) was added dropwise to a stirred, cooled (0°C) solution of p-toluenesulfonyl chloride (9.53g, 50.0mmol) in dry pyridine (30ml). The mixture was allowed to warm to room temperature and stirred overnight. The mixture was poured into water and the product was extracted into diethyl ether twice. The combined ethereal extracts were washed with 10% HCl twice and dried over anhydrous $MgSO_4$. The solvent was evaporated off and the remained crude product was purified by column chromatography (silica gel; hexane-ethyl acetate 10:1 and 5:1) to give a colorless liquid (8.88g, 97.2%). Purity >99% (HPLC). ^{1}H-NMR ($CDCl_3$, TMS, δ, ppm): 0.88 (t, J=6.4Hz, 3H, $C\underline{H}_3CH_2$-), 0.90 (d, J=6.0Hz, 3H, -CH($C\underline{H}_3$)-), 1.08-1.31, 1.31-1.52 (m, 2H, $CH_3C\underline{H}_2$-), 1.52-1.78 (m, 1H, -C$\underline{H}$(CH_3)-), 2.45 (s, 3H, -Ph$C\underline{H}_3$), 4.15 (dd, J=23.3, 4.3Hz, 2H, -$C\underline{H}_2OSO_2$-), 4.51 (dq, J=49.1, 4.9Hz, 1H, -C$\underline{H}$F-), 7.37 (d, J=8.0Hz, 2ArH, o to -CH_3), 7.81 (d, J=8.0Hz, 2ArH, o to -SO_2-).

(2R, 3S)-2-Fluoro-3-Methylpentyl 4'-Hydroxybiphenyl-4-Carboxylate (12)

A mixture of **7** (7.80g, 28.4mmol), **11** (7.17g, 28.4mmol), TBAH (1.42g) and dry DMSO (100ml) was stirred at 80°C under nitrogen atmosphere for 20 hours. The resulting clear yellow solution was poured into water. The product was extracted into diethyl ether twice and the combined ethereal extracts were dried over anhydrous $MgSO_4$. The solvent was evaporated off and the remained crude product was purified by column chromatography (silica gel; hexane-ethyl acetate 4:1) to give a colorless solid which was recrystallized from hexane-ethyl acetate (40:1) to yield colorless crystals (5.77g, 64.3%). Purity >99% (HPLC). mp 95.4°C (DSC). ^{1}H-NMR ($CDCl_3$, TMS, δ, ppm): 0.96 (t, J=7.0Hz, 3H, $C\underline{H}_3CH_2$-), 1.04 (d, J=6.7Hz, 3H, -CH($C\underline{H}_3$)-), 1.20-1.48, 1.48-1.67 (m, 2H, $CH_3C\underline{H}_2$-), 1.67-2.07 (m, 1H, -C$\underline{H}$(CH_3)-), 4.40-4.67, 4.79-4.91 (m, 3H, -C$\underline{H}$F$C\underline{H}_2$OCO-), 4.85 (bs, 1H, -PhO$\underline{H}$), 6.96 (d, J=8.7Hz, 2ArH, o to -OH), 7.52 (d, J=8.7Hz, 2ArH, m to -OH), 7.61 (d, J=8.5Hz, 2ArH, m to -COO-), 8.11 (d, J=8.5Hz, 2ArH, o to -COO-).

(2R,3S)-2-Fluoro-3-Methylpentyl 4'-(11-Vinyloxyundecanyloxy)biphenyl-4-Carboxylate (15)

A mixture of **12** (4.50g, 14.2mmol), anhydrous K_2CO_3 (4.91g, 35.5mmol) and acetone (90ml) was stirred at 60°C under nitrogen atmosphere for 2 hours. To the resulting yellow solution was added a solution of **14** (3.94g, 14.2mmol) in dry DMSO (5.0ml) and stirring was continued at 60°C for 20 hours. The mixture was poured into water and the product was extracted into diethyl ether twice. The combined ether extracts were dried over anhydrous $MgSO_4$. The solvent was evaporated off and the remained crude product was purified by column chromatography twice (silica gel; hexane-ethyl acetate 30:1, 20:1 and 10:1) to yield a white solid (4.23g, 58.1%). Purity >99% (HPLC). The thermal transition temperatures (°C) are: K 52.1 S_A 60.5 I on heating and I 52.9 S_A 38.9 S_C^* 19.7 K on cooling (DSC). ^{1}H-NMR ($CDCl_3$, TMS, δ, ppm): 0.97 (t, J=7.9Hz, 3H, $C\underline{H}_3CH_2$-), 1.04 (d, J=7.0Hz, 3H, -CH($C\underline{H}_3$)-), 1.31 (bs, 15H, $CH_3C\underline{H}_2$-, CH_2=CHO$CH_2CH_2(C\underline{H}_2)_7$-), 1.54-1.71 (m, 3H, $CH_3C\underline{H}_2$-, CH_2=CHO$CH_2C\underline{H}_2$-), 1.71-1.99 (m, 3H, -C$\underline{H}$(CH_3)-, -$C\underline{H}_2CH_2$OPh-), 3.67 (t, J=6.5Hz, 2H, CH_2=CHO$C\underline{H}_2$-), 3.97 (dd, J=6.9, 1.9Hz, 1H, $C\underline{H}_2$=CHO- trans), 4.00 (t, J=6.5Hz, 2H, -$C\underline{H}_2$OPh-), 4.17 (dd, J=14.3, 1.9Hz, 1H, $C\underline{H}_2$=CHO- cis), 4.37-4.67, 4.78-4.88 (m, 3H, -C$\underline{H}$F$C\underline{H}_2$O-), 6.48 (dd, J=14.3, 6.9Hz, 1H, CH_2=C$\underline{H}$O-), 6.99 (d, J=8.8Hz, 2ArH, o to -$(CH_2)_{11}$O-), 7.57 (d, J=8.8Hz, 2ArH, m to -$(CH_2)_{11}$O-), 7.64 (d, J=8.5Hz, 2ArH, m to -COO-), 8.11 (d, J=8.5Hz, 2ArH, o to -COO-).

(2S, 3S)-2-Fluoro-3-Methylpentanoic Acid (8)[10a, 11]

Precooled (0°C) dry pyridine (60ml) was added dropwise to pyridinium poly(hydrogen fluoride) (HF 70% by weight, 100g) in a Teflon flask at 0°C. L-Isoleucine (7.87g, 60.0mmol) was dissolved in this solution and $NaNO_2$ (6.21g, 90.0mmol) was added in three portions over a period of 30 min at 0°C with vigorous stirring. The reaction mixture was allowed to warm to room temperature and stirring was continued for 5 hours. The mixture was poured into water and the product was extracted into diethyl ether three times using a Teflon separatory funnel. The combined ethereal extracts were dried over anhydrous $MgSO_4$. The solvent was evaporated off and the remained crude product was distilled under vacuum to yield a slightly yellow liquid (2.22g, 27.6%); bp 78-80°C at 4mmHg. ^{1}H-NMR (DMSO-d_6, TMS, δ, ppm): 0.89 (t, J=7.3Hz, 3H, $C\underline{H}_3CH_2$-), 0.97 (d, J=7.0Hz, 2H, -CH($C\underline{H}_3$)-), 1.06-1.32, 1.32-1.56 (m, 2H, $CH_3C\underline{H}_2$-), 1.71-2.13 (m, 1H, -C$\underline{H}$(CH_3)-), 4.81 (dd, J=48.8, 4.0Hz, 1H, -C$\underline{H}$F-).

(2S, 3S)-2-Fluoro-3-Methylpentanol (9)

9 was synthesized by the same procedure as the one used for the preparation of **6**. Starting from 4.50g (33.5mmol) of **8**, 2.52g (67.0mmol) of $LiAlH_4$ and 80ml of dry THF, 2.40g (59.6%) of **9** was obtained as a colorless liquid. ^{1}H-NMR ($CDCl_3$, TMS, δ, ppm): 0.90 (d, J=6.8Hz, 3H, -CH($C\underline{H}_3$)-), 0.93 (t, J=7.1Hz, 3H, $C\underline{H}_3CH_2$-), 1.09-1.37, 1.47-1.90 (m, 3H, $CH_3C\underline{H}_2C\underline{H}(CH_3)$-), 2.48 (s, 1H, -$CH_2O\underline{H}$), 3.61-3.85 (m, 2H, -$C\underline{H}_2$OH), 4.15-4.29, 4.40-4.53 (m 1H, -C$\underline{H}$F-).

(2S, 3S)-2-Fluoro-3-Methylpentyl Tosylate (10)

10 was synthesized by the same procedure as the one used for the preparation of **7**. Starting from 1.80g (15.0mmol) of **7**, 4.38g (23.0mmol) of p-toluenesulfonyl chloride and 25ml of dry pyridine, 3.88g (94.3%) of **10** was obtained as a colorless liquid. Purity 98.0% (HPLC). ^{1}H-NMR ($CDCl_3$, TMS, δ, ppm): 0.86 (d, J=7.3Hz, 3H, -CH($C\underline{H}_3$)-), 0.88 (t, J=7.8Hz, 3H, $C\underline{H}_3CH_2$-), 1.09-1.32, 1.42-1.62 (m, 2H, $CH_3C\underline{H}_2$-), 1.62-1.89 (m, 1H, -C$\underline{H}$(CH_3)-), 2.46 (s, 3H, -Ph$C\underline{H}_3$), 4.00-4.35, 4.47-4.59 (m, 3H, -C$\underline{H}$F$C\underline{H}_2$O-), 7.37 (d, J=8.1Hz, 2ArH, o to -CH_3), 7.81 (d, J=8.1Hz, 2ArH, o to -SO_2-).

(2S, 3S)-2-Fluoro-3-Methylpentyl 4'-Hydroxybiphenyl-4-Carboxylate (13)

13 was synthesized by the same procedure as the one used for the preparation of **12**. Starting from 3.00g (10.9mmol) of **10**, 2.52g (10.0mmol) of **11**, 0.50g of TBAH and 40ml of dry DMSO, 2.27g (71.7%) of **13** was obtained as colorless crystals. Purity >99% (HPLC). mp 127.5°C (DSC). ^{1}H-NMR ($CDCl_3$, TMS, δ, ppm): 0.97 (t, J=7.7Hz, 3H, $C\underline{H}_3CH_2$-), 1.00

(d, J=7.1Hz, 3H, -CH($C\underline{H}_3$)-), 1.19-1.45, 1.45-1.75 (m, 2H, $CH_3C\underline{H}_2$-), 1.75-2.03 (m, 1H, -$C\underline{H}(CH_3)$-), 4.33-4.90 (m, 3H, -$C\underline{H}FC\underline{H}_2O$-), 5.59 (bs, 1H, -PhO$\underline{H}$), 6.95 (d, J=8.6Hz, 2ArH, o to -OH), 7.53 (d, J=8.6Hz, 2ArH, m to -OH), 7.62 (d, J=8.2Hz, 2ArH, m to -COO-), 8.11 (d, J=8.2Hz, 2ArH, o to -COO-).

(2S, 3S)-2-Fluoro-3-Methylpentyl 4'-(11-Vinyloxyundecanyloxy)biphenyl-4-Carboxylate (16)

Monomer **16** was synthesized by the same procedure as the one used for the preparation of **15**. Starting from 1.94g (6.1mmol) of **13**, 1.66g (6.0mmol) of **14**, 2.11g (15.3mmol) of anhydrous K_2CO_3, 2.5ml of dry DMSO and 50ml of acetone, 1.28g (40.8%) of **16** was obtained as a white solid. Purity >99% (HPLC). The thermal transition temperatures (°C) are: K 54.7 S_A 60.2 I on heating, and I 54.6 S_A 39.8 S_C^* 20.7 K on cooling (DSC). ^{1}H-NMR ($CDCl_3$, TMS, δ, ppm): 0.97 (t, 7.4 Hz, 3H, $C\underline{H}_3CH_2$-), 1.00 (d, J=6.9Hz, 3H, -CH($C\underline{H}_3$)-), 1.31 (bs, 15H, $CH_3C\underline{H}_2$-, CH_2=$CHOCH_2CH_2(C\underline{H}_2)_7$-), 1.56-1.72 (m, 3H, $CH_3C\underline{H}_2$-, CH_2=$CHOCH_2C\underline{H}_2$-), 1.72-2.00 (m, 3H, -$C\underline{H}(CH_3)$-, -$C\underline{H}_2CH_2OPh$-), 3.67 (t, J=6.6Hz, 2H, CH_2=$CHOC\underline{H}_2$-), 3.97 (dd, J=6.9, 1.9Hz, 1H, $C\underline{H}_2$=CHO- trans), 4.01 (t, J=6.5Hz, 2H, -$C\underline{H}_2OPh$-), 4.17 (dd, J=14.1, 1.9Hz, 1H, $C\underline{H}_2$=CHO- cis), 4.29-4.79 (m, 3H, -$C\underline{H}FC\underline{H}_2O$-), 6.48 (dd, J=14.1, 6.9Hz, 1H, CH_2=$C\underline{H}O$-), 6.99 (d, J=8.8Hz, 2ArH, o to -$(CH_2)_{11}O$-), 7.57 (d, J=8.8Hz, 2ArH, m to -$(CH_2)_{11}O$-), 7.63 (d, J=8.5Hz, 2ArH, o to -COO-), 8.11 (d, J=8.5Hz, 2ArH, m to -COO-).

Cationic Polymerizations

Polymerizations were carried out in a three-necked round bottom flask equipped with a Teflon stopcock and rubber septa under argon atmosphere at 0°C for 1 hour. All glassware was dried overnight at 140°C. The monomer was further dried under vacuum overnight in the polymerization flask. After the flask was filled with argon, freshly distilled dry CH_2Cl_2 was added via a syringe and the solution was cooled to 0°C. $S(CH_3)_2$ and CF_3SO_3H were then added via a syringe. The monomer concentration was about 0.224 M and the $S(CH_3)_2$ concentration was 10 times larger than that of CF_3SO_3H. The polymer molecular weight was controlled by the monomer/initiator ($[M]_o/[I]_o$) ratio. After quenching the polymerization with a mixture of NH_4OH and methanol (1:2), the reaction mixture was poured into methanol to give a white precipitate. The obtained polymer was purified by reprecipitation (chloroform solution, methanol) and dried under vacuum.

Results and Discussion

Determination of the optical purities of monomers 15 and 16

The synthesis of two diastereomeric monomers **15** and **16** is outlined in Scheme 1. The starting material, L-isoleucine (**1**), is one of the naturally occurring α-amino acids and has (2S, 3S) configurations at the two chiral centers. In the course of transformation of L-isoleucine **1** into the fluorinated ester **5** and subsequently into the fluorinated acid **8**, the amino group of L-isoleucine was first converted into a hydroxy group[10] (compound **2**) and a fluorine atom[11] (compound **8**) respectively via a diazonium salt. These substitution reactions proceed with the retention of configuration at the C2 position because of the anchimeric assistance of the carboxylate group.[11] Compound **2** was further converted into triflate **4** which was substituted with a fluorine atom by using n-Bu_4NF.[10] As this substitution reaction proceeds with Walden inversion of configuration at the C2 chiral center, compound **5** is expected to have (2R, 3S) configurations, while compounds **8** has (2S, 3S) configurations. Compounds **5** and **8** are expected to be transformed into monomers **15** and **16** without any change of their configurations during the other steps of the synthesis.

The 200 MHz ^{1}H-NMR spectra of monomers **15** and **16** are shown in Figure 1. Figure 2 presents the 200 MHz ^{1}H-NMR spectra of corresponding homopolymers, poly(**15**) (DP=6.0) and poly(**16**) (DP=5.5). These two figures clearly demonstrate that the signals due to the k and the l protons (4.3-4.8ppm) differ in their splitting patterns from each other between monomers **15** and **16**, and between polymers poly(**15**) and poly(**16**). The peaks of poly(**15**) and poly(**16**) are similar to those of monomers **15** and **16** respectively, although the polymers show broadened peaks.

In order to elucidate the assignment of these peaks ^{19}F decoupled ^{1}H-NMR analysis was performed by using 300 MHz NMR spectroscopy. Figure 3 presents the ^{19}F decoupled ^{1}H-NMR spectra (top) and the normal ^{1}H-NMR spectra (bottom) for the k and the l protons of monomers **15**, **16** and polymers poly(**15**) and poly(**16**). In the ^{19}F decoupled spectra the peaks show an AMNX pattern where A corresponds to the l proton, MN corresponds to the two k protons and X corresponds to the fluorine atom. For **15** and poly(**15**) A (the l proton) can be assigned to the peaks at 4.71ppm and MN (the two k protons) can be assigned to the peaks at 4.53ppm and 4.45ppm, while for **16** and poly(**16**) A and M can be assigned to the peaks at 4.52-4.70ppm and N can be assigned to the peaks at 4.44ppm. Thus it is demonstrated that these two pairs of diastereomers have different structures and each diastereomer is expected to have high optical purity.

The optical purity arising from the C2 chiral center was successfully determined by a ^{19}F-NMR technique. The results are summarized in Figure 4. These spectra exhibit two clear clusters at -63.0ppm and at -69.5ppm and it is obvious that the former corresponds to

2S configuration and the latter corresponds to 2R configuration. The optical purities calculated from the integration of these two clusters are 2R 96% (92%ee) for monomer **15** and 2S 98% (96%ee) for monomer **16**. The corresponding polymers poly(**15**) and poly(**16**) have the optical purity of 2R 98% (96%ee) and 2S 98% (96%ee) respectively, and it is demonstrated that no racemization has occurred at the C2 chiral center during the polymerization.

The optical purity arising from the C3 chiral center was not determined because the signal of the m proton was burried under the large signals due to the alphatic spacer and the terminal alkyl chains. However it is believed that the original optical purity of L-isoleucine is maintained at the C3 chiral center because of its chemical stability.

Homopolymerization of 15 and 16

The homopolymerizations of **15** and **16** are presented in Scheme 2. All polymerizations were carried out at 0°C in CH_2Cl_2 by a living cationic polymerization technique using $CF_3SO_3H/(CH_3)_2S$ as an initiation system. Previous work in our laboratory[12] and others[14] has shown that the CF_3SO_3H initiated polymerization of vinyl ethers in the presence of a Lewis base such as $(CH_3)_2S$ gives well defined polymers with controlled molecular weights and narrow polydispersities. The polymerization mechanism is discussed in detail in previous publications.[9, 12, 13]

The characterization of poly(**15**) and poly(**16**) by gel permeation chromatography (GPC) and differential scanning calorimetry (DSC) is summarized in Tables I and II respectively. The low polymer yields are the result of the loss of polymer during purification. Relative number-average molecular weights of polymers determined by GPC exhibit a linear dependence on the initial concentration ratio of monomer to initiator ($[M]_o/[I]_o$) as shown in Figure 5. All polydispersities are less than 1.20. The $[M]_o/[I]_o$ ratio provides a very good control of the polymer molecular weight. All these features demonstrate the typical characteristics of the living polymerization mechanism. The absolute number-average molecular weights were difficult to determine by ^{1}H-NMR spectroscopy from the chain ends of the polymer owing to signal overlap.

The mesomophic behaviors of poly(**15**) and poly(**16**) were investigated by DSC and thermal optical polarized microscopy. Figures 6 and 7 present the DSC thermograms of poly(**15**) and poly(**16**) with various degrees of polymerization (DP) respectively. The phase behaviors of the two diastereomeric homopolymers can be compared by superimposing the plotts of the dependencies of their thermal transition temperatures as a function of DP (Figure 8). As observed from this figure the phase behavior of poly(**15**) is identical to that of poly(**16**). The DSC curves of first heating scan differ from those of second heating scan

(Figures 6 and 7). However, second and subsequent heating scans exhibit identical DSC traces. First and subsequent cooling scans also exhibit identical DSC traces. On the first heating scan all polymers exhibit a crystalline phase. In polymers with DP≤8.3 the crystalline phase melts into a S_C^* phase which is followed by S_C^*-S_A and S_A-I phase transitions. In polymers with DP≥8.4 another higher order smectic phase (S_X) is observed between K and S_C^* phases. The nature of this S_X phase was not identified. On the second heating and cooling scans all polymers exhibit the S_X-S_C^*-S_A-I phase sequence. The polymers with DP≤6.0 have an additional crystalline phase. Especially polymers with DP=3.4 crystallize on the second heating scan. This represents a classic example of the "polymer effect" which shows how the kinetically controlled crystallization process affects the stability of the thermodynamically controlled mesophase[13]. The low molecular weight polymers exhibit a high rate of crystallization and therefore, can crystallize on the second heating scan, while the higher molecular weight polymers have much lower rate of crystallization and, subsequently, they do not crystallize on the second heating scan. Similar examples of this behavior are available both from our[9a, 12a, 15] and from other laboratories.[16]

Representative optical polarized micrographs of the texture exhibited by the S_A and the S_C^* phases of poly(**15**) (DP=7.7) and the S_C^* and the S_X phases of poly(**16**) (DP=8.3) are presented in Figure 9.

Miscibility Studies

Monomers **15** and monomer **16** were mixed in various compositions and the phase behavior of their mixtures was investigated by DSC. Mixtures were prepared by dissolving the two monomers in CH_2Cl_2 followed by evaporation of the solvent under vacuum. The phase behavior of binary mixtures of poly(**15**) (DP=6.0) with poly(**16**) (DP=12.6) was also investigated in the same manner. The DSC thermograms of the monomer and the polymer mixtures are presented in Figures 10 and 11 respectively. The thermal transition temperatures collected from these DSC themograms are summarized in Tables III and IV. In Figures 12 and 13 the transition temperatures are plotted as a function of the composition of the binary mixtures.

The phase behavior of monomer **15** is identical to that of monomer **16**. Both monomers display enantiotropic S_A, montropic S_C^* and crystalline phases, while the corresponding polymers display enantiotropic S_A, S_C^* and S_X mesophases. Upon mixing the crystalline phase of the monomer system was suppressed and an eutectic was observed. The theoretical temperatures for the K-S_A (the first and the second heating scans) and S_C^*-K (the first cooling scan) transitions were calculated from the Schröder-van Laar equation[17, 18] for an ideal solution and are also plotted in Figure 12. The theoretical values show a linear

dependence of composition and are in contrast to the experimental values which show an eutectic composition. In the S_C^* and S_A mesophases, on the contrary, the two diastereomeric structural units of the monomer system are miscible and isomorphic across the full composition range and all transition temperatures show a linear dependence on composition.

In the polymer mixtures the two diastereomeric structural units are miscible and isomorphic within all their mesophases and over the entire range of composition. Since the degrees of polymerization of poly(**15**) and poly(**16**) used for the preparation of the polymer mixtures are different, the phase diagrams in Figure 13 show linear dependences. The theoretical transition temperatures for the S_A-I transition were calculated by the Schröder-van Laar equation and are plotted in Figure 13. As observed from this figure the experimental data are in good agreement with the theoretical values.

A representative texture of the S_C^* mesophase displayed by the binary mixture of poly(**15**) (DP=6.0) with poly(**16**) (DP=12.6) (50/50) is presented in Figure 14.

Copolymerization of 15 with 16

Copolymerization of **15** with **16** was performed to cover the entire range of compositions . Attempts were made to synthesize poly(**15**-*co*-**16**) with DP=16. Since the transition temperatures of polymers are strongly dependent on their molecular weights, it is essential to synthesize polymers having identical molecular weights in order to compare their transition temperatures. This can be achieved only by a living polymerization. The copolymerization results are listed in Table V. The yields reported in Table V are lower than quantitative due to polymer losses during the purification process. However, all conversions were quantitative and therefore, the copolymer composition is identical to that of the monomer feed[13b]. The number-average molecular weights determined by GPC are *ca.* 12.

The first and the second heating, and the first cooling DSC traces of all polymers and copolymers are presented in Figure 15. The thermal transition temperatures collected from Figure 15 are summarized in Table V and plotted against copolymer composition in Figure 16. In Figure 17 the S_A-I transition temperatures obtained during the first heating scans are compared with those calculated from the Schröder-van Laar equation for an ideal solution. The copolymers poly(**15**-*co*-**16**) exhibit the same phase behavior as their parent homopolymers over the entire range of compositions. The isotropization temperatures of the copolymers are identical to those predicted by the Schröder-van Laar equation, although there are slight deviations due to the molecular weight fluctuation of the copolymers. These results demonstrate that the two diastereomeric structural units of **15** and **16** are isomorphic within their enantiotropic S_A, S_C^* and S_X mesophases and behave as an ideal solution in the

copolymer. A representative texture of the S_C^* mesophase displayed by poly(**15**-*co*-**16**) (50/50) with DP=12.0 is presented in Figure 18.

Isomorphism of 15 with 16 and of their homopolymers and copolymers

The phase behaviors of **15** and poly(**15**) are identical to those of **16** and poly(**16**) respectively. Miscibilty studies and copolymerization studies revealed that the two structural units derived from the diastereomeric monomers **15** and **16** are isomorphic[19] and form ideal solutions within all liquid crystalline phases over the entire range of compositions. Within experimental error no chiral molecular recognition between the 2R and the 2S stereogenic centers has been observed in their liquid crystalline phases since no deviation from ideal solution behavior was observed at their 50/50 composition. The only exception is the crystalline phase exhibited by the monomer mixtures where crystallization temperatures are suppressed to show an eutectic composition. Since the physical properties of diasteromers are most frequently different, these results are of unusual interest.

The synthesis and the phase behavior of two low molar mass diastereomeric liquid crystals, 4'-(n-dodecanyloxy)-4-biphenylyl 2-fluoro-3-methylpentanoate (**17**), were reported by Arakawa et al.[10a] Their structures are related to those of monomers investigated in the present paper. The major difference between **17** and our monomers **15** and **16** is that **17** is based on 4, 4'-dihydroxybiphenyl mesogen whereas **15** and **16** are based on 4'-hydroxybiphenyl-4-carboxylate mesogen. It should be noted that the phase behaviors of (2R, 3S)-**17** and (2S, 3S)-**17** are quite different, i.e., (2R, 3S)-**17** exhibits S_C^* and S_A phases, while (2S, 3S)-**17** exhibits only a S_A phase.

The phase diagram of binary mixtures of enantiomeric liquid crystals as a function of enantiomeric excess was investigated for some antiferroelectric liquid crystals.[5] In all these studies, with decreasing enantiomeric excess the temperature range of S_C^* phase increases whereas the temperature range of $S_{C_A}^*$ (antiferroelectric S_C^* phase) decreases. However no attention is paid to the isotropization temperature and no quantitative data are available. Chiral molecular recognition between two enantiomeric antipodes is observed in liquid crystals with a chorine atom on their chiral centers.[4c, d] In these examples racemic mixtures show a higher isotropization temperature than that of the optically active enantiomers. The temperature difference is only 3°C[4d] or even less than 1°C.[4c] Bahr et al. attributed this temperature shift to steric packing effects of chiral moiety.[4c] They also reported that for transitions involving chiral smectic phases (e.g., S_C-S_A, S_G-S_C, S_G-S_A) dependence of the transition temperature on chirality was observed, whereas for transitions between two non-chiral smectic phases (e.g., S_B-S_A, S_E-S_B) no dependence of the transition temperature on chirality was observed.[4b, c]

Currently we have no definitive explanation for the absence of chiral recognition in these liquid crystalline systems. However, it is possible to speculate that the less bulky fluorine atom of the chiral center compared to the chlorine atom is responsible for the absence of chiral recognition.

Acknowledgment

Financial support by the Office of Naval Research and Asahi Chemical Industry Co., Ltd., Japan is gratefully acknowledged.

References and Notes

(1) (a) Arnett, E. M.; Harvey, N. G.; Rose, P. L. *Acc. Chem. Res.* **1989**, *22*, 131. (b) Pirkle, W. H.; Pochapsky, T. C. *Chem. Rev.* **1989**, *89*, 347. (c) Jacques, J.; Collet, A. ...en, S. H. *Enantiomers, Racemates and Resolutions*; Krieger Publishing Co.: Mal... 1991.

(2) (a) Arnett, E. M.; Thompson, O. *J. Am. Chem. Soc.* **1981**, *103*, 968. (b) Harvey, N. G.; Rose, P. L.; Mirajovsky, D.; Arnett, E. M. *J. Am. Chem. Soc.* **1990**, *112*, 3547.

(3) Arnett, E. M.; Gold, J. M. *J. Am. Chem. Soc.* **1982**, *104*, 636.

(4) (a) Leclercq, M.; Billard, J.; Jacques, J. *Mol. Cryst. Liq. Cryst.* **1969**, *8*, 367. (b) Bahr, CH.; Heppke, G.; Sabaschus, B. *Ferroelectrics* **1988**, *84*, 103. (c) Bahr, CH.; Heppke, G.; Sabaschus, B. *Liq. Cryst.* **1991**, *9*, 31. (d) Slaney, A. J.; Goodby, J. W. *Liq. Cryst.* **1991**, *9*, 849.

(5) (a) Yamada, Y.; Mori, K.; Yamamoto, N.; Hayashi, H.; Nakamura, K.; Yamawaki, M.; Orihara, H.; Ishibashi, Y. *Jpn. J. Appl. Phys.* **1989**, *28*, L1606. (b) Takezoe, H.; Lee, J.; Chandani, A. D. L.; Gorecka, E.; Ouchi, Y.; Fukuda, A.; Terashima, K.; Furukawa, K. *Ferroelectrics* **1991**, *114*, 187. (c) Takezoe, H.; Fukuda, A.; Ikeda, A.; Takanishi, Y.; Umemoto, T.; Watanabe, J.; Iwane, H.; Hara, M.; Itoh, K. *Ferroelectrics* **1991**, *122*, 167.

(6) (a) Harvey, N.; Rose, P.; Porter, N. A.; Huff, J. B.; Arnett, E. M. *J. Am. Chem. Soc.* **1988**, *110*, 4395. (b) Heath, J. G.; Arnett, E. M. *J. Am. Chem. Soc.* **1992**, *114*, 4500.

(7) (a) Burdon, J.; Farazmand, I.; Stacey, M.; Tatlow, J. C. *J. Chem. Soc.* **1957**, 2574. (b) Stang, P. J.; Hanack, M.; Subramanian, L. R. *Synthesis* **1982**, 85. (c) Beard, C. D.; Baum, K.; Grakauskas, V. *J. Org. Chem.* **1973**, *38*, 3673.

(8) Dungan, C. H.; Van Wazer, J. R. *Compilation of Reported ^{19}F NMR Chemical Shifts*; Wiley-Interscience: New York, 1970.

(9) (a) Percec, V.; Zheng, Q.; Lee, M. *J. Mater. Chem.* **1991**, *1*, 611. (b) Percec, V.; Zheng, Q.; Lee, M. *J. Mater. Chem.* **1991**, *1*, 1015. (c) Percec, V.; Zheng, Q. *J. Mater. Chem.* **1992**, *2*, 475. (d) Percec, V.; Zheng, Q. *J. Mater. Chem.* **1992**, *2*, 1041.

(10) (a) Arakawa, S.; Nito, K.; Seto, J. *Mol. Cryst. Liq. Cryst.* **1991**, *204*, 15. (b) Chan, L. K. M.; Gray, G. W.; Lacey, D.; Scrowston, R. M.; Shenouda, I. G. *Mol. Cryst. Liq. Cryst.* **1989**, *172*, 125.

(11) (a) Olah, G. A.; Welch, J. *Synthesis* **1974**, 652. (b) Olah, G. A.; Welch, J. T.; Vankar, Y. D.; Nojima, M.; Kerekes, I.; Olah, J. A. *J. Org. Chem.* **1979**, *44*, 3872. (c) Keck, R.; Rétey, J. *Helv. Chim. Acta* **1980**, *63*, 769. (d) Olah, G. A.; Prakash, G. K.; Chao, Y. L. *Helv. Chim. Acta* **1981**, *64*, 2528. (e) Faustint, F.; Munari, S. D.; Panzeri, A.; Villa, V.; Gandolfi, C. A. *Tetrahedron Lett.* **1981**, *22*, 4533. (f) Barber, J.; Keck, R.; Rétey, J. *Tetrahedron Lett.* **1982**, *23*, 1549.

(12) (a) Percec, V.; Lee, M.; Jonsson, H. *J. Polym. Sci., Polym. Chem. Ed.* **1991**, *29*, 327. (b) Percec, V.; Lee, M. *Macromolecules* **1991**, *24*, 1017.

(13) (a) Percec, V.; Lee, M.; Rinaldi, P.; Litman, V. E. *J. Polym. Sci., Polym. Chem. Ed.* **1992**, *30*, 1213. (b) for a brief review on the molecular engineering of side chain LCP by living cationic polymerization see: Percec, V., Tomazos, D., *Adv. Mater.*, **1992**, *4*, 548.

(14) (a) Cho, C. G.; Feit, B. A.; Webster, O. W. *Macromolecules* **1990**, *23*, 1918. (b) Cho, C. G.; Feit, B. A.; Webster, O. W. *Macromolecules* **1992**, *25*, 2081. (c) Lin, C. H.; Matyjaszewsky, K. *Polym. Prepr., Am. Chem. Soc. Div. Polym. Chem.* **1990**, *31*, 599.

(15) (a) Percec, V.; Tomazos, D.; Pugh, C. *Macromolecules* **1989**, *22*, 3259. (b) Rodriguez-Parada, J. M.; Percec, V. *J. Polym. Sci., Polym. Chem. Ed.* **1986**, *24*, 1363. (c) Rodenhouse, R.; Percec, V.; Feiring, A. E. *J. Polym. Sci., Polym. Lett. Ed.* **1990**, *28*, 345. (d) Percec, V.; Lee, M. *Macromolecules* **1991**, *24*, 2780. (e) Percec, V.; Lee, M. *Polymer* **1991**, *32*, 2862. (f) Percec, V.; Lee, M. *Polym. Bull.* **1991**, *25*, 123. (g) Jonsson, H.; Percec, V.; Hult, A. *Polym. Bull.* **1991**, *25*, 115. (h) Percec, V.; Gomes, A. D. S.; Lee, M. *J. Polym. Sci., Polym. Chem. Ed.* **1991**, *29*, 1615. (i) Percec, V.; Wang, C. S. *Polym. Bull.* **1991**, *26*, 15.

(16) (a) Sagane, T.; Lenz, R. W. *Polym. J.* **1988**, *20*, 923. (b) Sagane, T.; Lenz, R. W. *Polymer* **1989**, *30*, 2269. (c) Sagane, T.; Lenz, R. W. *Macromolecules* **1989**, *22*, 3763.

(17) (a) Van Hecke, G. R. *J. Phys. Chem.* **1979**, *83*, 2344. (b) Achard, M. F.; Mauzac, M.; Richard, H.; Sigaud, G.; Hardouin, F. *Eur. Polym. J.* **1989**, *25*, 593.

(18) (a) Percec, V.; Lee, M. *J. Mater. Chem.* **1991**, *1*, 1007. (b) Percec, V.; Lee, M.; Zheng, Q. *Liq. Cryst.* **1992**, *12*, 715. (c) Percec, V; Johansson, G. *J. Mater. Chem.* **1993**, *3*, 83.

(19) Percec, V.; Tsuda, Y. *Polymer*, **1991**, *32*, 661.

Scheme and Figure Captions

Scheme 1. Synthesis of monomers **15** and **16**.

Scheme 2. Cationic polymerization of **15** and **16**.

Figure 1. ^{1}H-NMR spectra of monomers. (a) **15**; (b) **16**.

Figure 2. ^{1}H-NMR spectra of polymers. (a) Poly(**15**) (DP=6.0); (b) poly(**16**) (DP=5.5).

Figure 3. ^{19}F decoupled ^{1}H-NMR spectra (top) and normal ^{1}H-NMR spectra (bottom) of monomers and polymers. (a) **15**; (b) **16**; (c) poly(**15**) (DP=6.0); (d) poly(**16**) (DP=5.5).

Figure 4. ^{19}F-NMR spectra of monomers and polymers. (a) **15**; (b) **16**; (c) poly(**15**) (DP=6.0); (d) poly(**16**) (DP=5.5).

Figure 5. The dependence of the number-average molecular weight (Mn) and polydispersity (Mw/Mn) determined by GPC on the $[M]_o/[I]_o$ ratio.

Figure 6. DSC thermograms (20°C/min) of poly(**15**) with different DP. (a) First heating scans; (b) second heating scans; (c) first cooling scans.

Figure 7. DSC thermograms (20°C/min) of poly(**16**) with different DP. (a) First heating scans; (b) second heating scans; (c) first cooling scans.

Figure 8. The dependence of phase transition temperatures on the degree of polymerization of poly(**15**) (open) and poly(**16**) (closed). (a) Data from the first heating scans; (b) data from the second heating scans; (c) data from the first cooling scans.

Figure 9. Representative optical polarized micrographs of: (a) the S_A mesophase displayed by poly(**15**) (DP=7.7) upon cooling to 100°C (100x); (b) the S_C* mesophase displayed by poly(**15**) (DP=7.7) upon cooling to 69°C (400x); (c) the S_C* mesophase displayed by poly(**16**) (DP=8.3) upon cooling to 85°C (400x); (d) the S_X mesophase displayed by poly(**16**) (DP=8.3) upon cooling to 43°C (400x).

Figure 10. DSC thermograms (20°C/min) of the binary mixtures of monomer **15** (X) with monomer **16** (Y). (a) First heating scans; (b) second heating scans; (c) first cooling scans.

Figure 11. DSC thermograms (20°C/min) of the binary mixtures of poly(**15**) (DP=6.0) (X) with poly(**16**) (DP=12.6) (Y). (a) First heating scans; (b) second heating scans; (c) first cooling scans.

Figure 12. The dependence of phase transition temperatures on the composition of the binary mixtures of **15** with **16**. (a) Data from the first heating scans; (b) data from the second heating scans; (c) data from the first cooling scans. (□, Δ, ○) Experimental data; (▲) data calculated by the Schröder-van Laar equation.

Figure 13. The dependence of phase transition temperatures on the composition of the binary mixtures of poly(**15**) (DP=6.0) with poly(**16**) (DP=12.6). (a) Data from the first heating scans; (b) data from the second heating scans; (c) data from the first cooling scans. (□, Δ, ○, ■, ●) Experimental data; (▲) data calculated by the Schröder-van Laar equation.

Figure 14. Representative optical polarized micrographs of the S_C^* mesophase displayed by the binary mixture of poly(**15**) (DP=6.0) with poly(**16**) (DP=12.6) (50/50) upon cooling to 72°C (400x).

Figure 15. DSC thermograms (20°C/min) of the copolymers of **15** (X) with **16** (Y). (a) First heating scans; (b) second heating scans; (c) first cooling scans.

Figure 16. The dependence of phase transition temperatures on the composition of poly(**15**-*co*-**16**) (DP=11.6~12.8). (a) Data from the first heating scans; (b) data from the second heating scans; (c) data from the first cooling scans.

Figure 17. The dependence of isotropization temperature on the composition of poly(**15**-*co*-**16**) (DP=11.6~12.8). Experimental data from the first heating scan (open); data calculated by the Schröder-van Laar equation (closed).

Figure 18. Representative optical polarized micrographs of the S_C^* mesophase displayed by poly(**15**-*co*-**16**) (50/50) with DP=12.0 upon cooling to 70°C (400x).

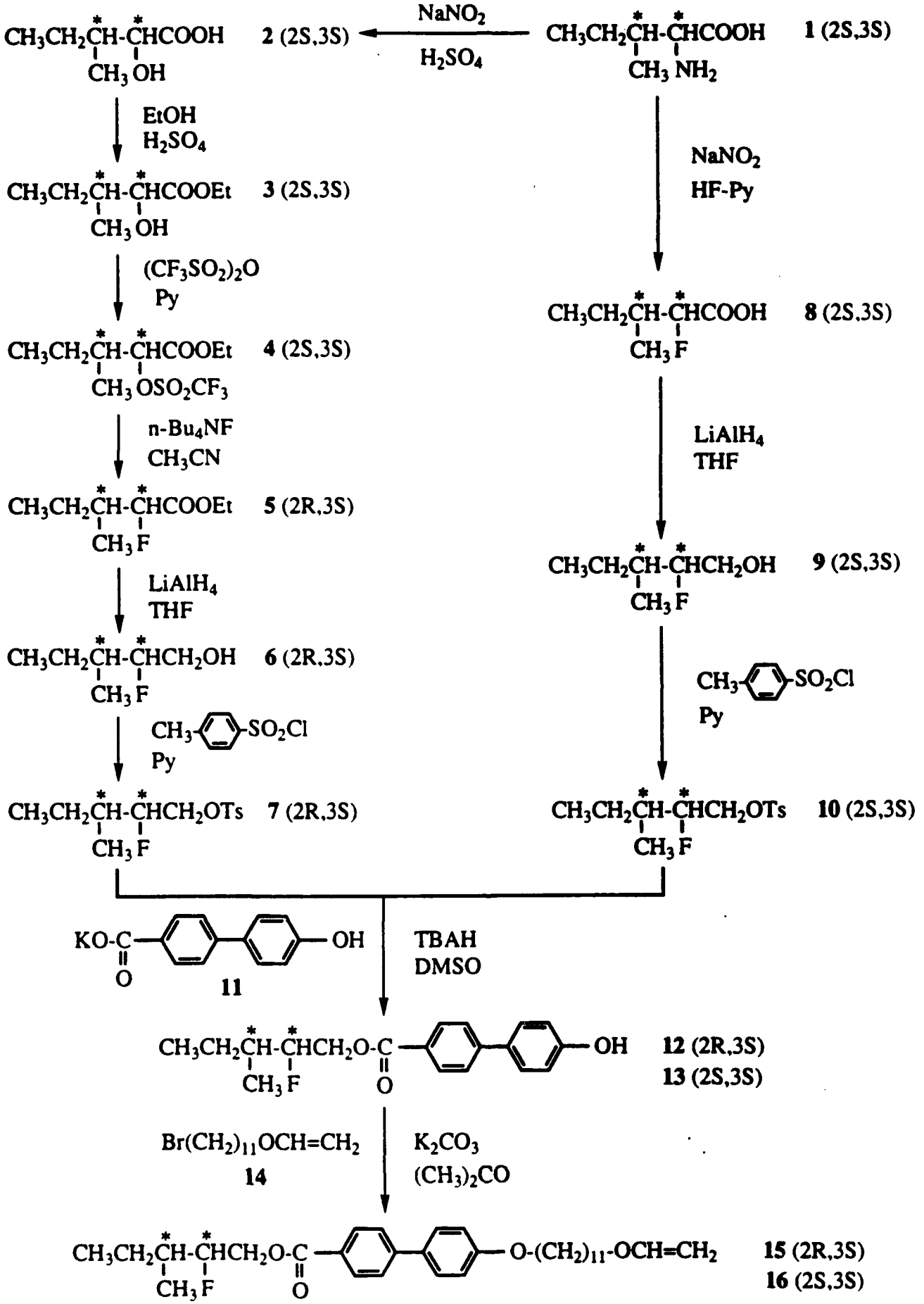
NaNO2
H2SO4
2 (2S,3S)
1 (2S,3S)
EtOH
H2SO4
3 (2S,3S)
(CF3SO2)2O
Py
4 (2S,3S)
n-Bu4NF
CH3CN
5 (2R,3S)
LiAlH4
THF
6 (2R,3S)
CH3-SO2Cl
Py
7 (2R,3S)
NaNO2
HF-Py
8 (2S,3S)
LiAlH4
THF
9 (2S,3S)
CH3-SO2Cl
Py
10 (2S,3S)
KO-C
O
OH
11
TBAH
DMSO
12 (2R,3S)
13 (2S,3S)
Br(CH2)11OCH=CH2
14
K2CO3
(CH3)2CO
O-(CH2)11-OCH=CH2
15 (2R,3S)
16 (2S,3S)

Scheme 1

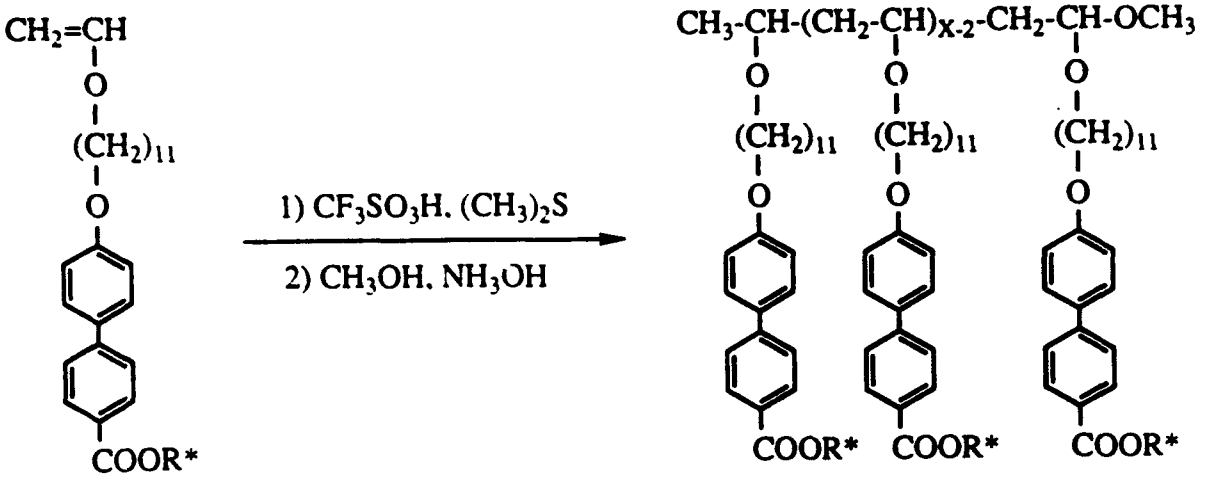

R*: $CH_2\overset{*}{C}H\overset{*}{C}HCH_2CH_3$ (F, CH_3)

15 (2R,3S)
16 (2S,3S)

Scheme 2

Table I. Cationic Polymerization of (2R, 3S)-2-Fluoro-3-Methylpentyl 4'-(11-Vinyloxyundecanyloxy)biphenyl-4-Carboxylate (15) and Characterization of the Resulting Polymers[a]

Sample No.	$[M]_o/[I]_o$	Polymer Yield(%)	$Mnx10^{-3}$	Mw/Mn	DP	Phase transitions (°C) and corresponding enthalpy changes (kcal/mru)[b]	
						heating	cooling
1	2	31.7	1.8	1.07	3.4	K 45.3(3.16) K 56.9(0.34) S_C^* 81.7(0.07) S_A 90.6(1.67) I	I 84.0(-1.62) S_A 76.4(-0.07) S_C^* 29.8(-0.40) S_X 18.2(-0.93) K
						S_X 36.2(0.82) K 55.3(1.99) S_C^* 80.5(0.07) S_A 89.8(1.65) I	
2	3	54.8	2.2	1.11	4.3	K 47.0(2.91) S_C^* 85.7(0.06) S_A 97.0(1.62) I	I 90.3(-1.58) S_A 81.0(-0.06) S_C^* 34.1(-0.45) S_X 20.7(-0.50) K
						K 34.5(0.59) S_X 38.6(0.52) S_C^* 85.3(0.07) S_A 96.4(1.64) I	
3	5	65.5	3.1	1.12	6.0	K 49.8(2.35) S_C^* 90.9(0.03) S_A 106.5(1.59) I	I 99.6 (-1.55) S_A 85.8(-0.06)S_C^* 41.6(-0.52) S_X 30.4(-0.31) K
						K 38.8(0.44) S_X 46.6(0.58) S_C^* 90.4(0.06) S_A 105.9(1.55) I	
4	8	80.1	4.0	1.13	7.7	K 54.0(2.09) S_C^* 94.3(0.03) S_A 116.1(1.57) I	I 109.5(-1.53) S_A 90.0(-0.06) S_C^* 48.9(-0.92) S_X
						K 49.7(0.32) S_X 54.1(0.81) S_C^* 94.2(0.05) S_A 115.9(1.57) I	
5	12	76.2	4.3	1.17	8.4	K 54.8(1.27) S_X 58.6(0.78) S_C^* 95.3(0.04) S_A 118.0(1.55) I	I 111.9(-1.49) S_A 90.9(-0.06) S_C^* 51.7(-1.05) S_X
						S_X 57.9(1.17) S_C^* 95.3(0.05) S_A 118.4(1.51) I	
6	20	82.4	6.2	1.20	12.1	K 58.2(0.72) S_X 64.8(1.05) S_C^* 97.6(0.05) S_A 126.4(1.45) I	I 120.0(-1.44) S_A 93.3(-0.06) S_C^* 59.0(-1.04) S_X
						S_X 64.7(1.15) S_C^* 97.5(0.04) S_A 126.2(1.45) I	
7	30	83.3	8.1	1.19	15.7	K 59.9(0.57) S_X 67.9(1.10) S_C^* 99.0(0.04) S_A 130.5(1.39) I	I 123.4(-1.39) S_A 94.0(-0.06) S_C^* 62.1(-1.13) S_X
						S_X 67.9(1.15) S_C^* 99.0(0.04) S_A 130.4(1.40) I	

[a] Polymerization temperature: 0°C; polymerization solvent: methylene chloride; $[M]_o$=0.224; $[Me_2S]_o/[I]_o$=10; polymerization time: 1hour.

[b] Data on first line are from first heating and cooling scans. Data on second line are from second heating scan.

Table II. Cationic Polymerization of (2S, 3S)-2-Fluoro-3-Methylpentyl 4'-(11-Vinyloxyundecanyloxy)biphenyl-4-Carboxylate (16) and Characterization of the Resulting Polymers[a]

Sample No.	$[M]_o/[I]_o$	Polymer Yield(%)	$Mn \times 10^{-3}$	Mw/Mn	DP	Phase transitions (°C) and corresponding enthalpy changes (kcal/mru)[b]	
						heating	cooling
1	2	46.1	1.8	1.06	3.4	K 43.5(2.60) K 55.6(0.86) S_C^* 78.0(0.06) S_A 86.9(1.64) I	I 80.8(-1.60) S_A 73.9(-0.06) S_C^* 28.0(-0.33) S_X 13.2(-0.61) K
						S_X 34.5(0.65) K 55.0(2.19) S_C^* 78.2(0.07) S_A 86.9(1.64) I	
2	3	54.0	2.1	1.10	4.1	K 45.9(2.81) S_C^* 83.3(0.06) S_A 93.3(1.65) I	I 87.2(-1.59) S_A 79.0(-0.06) S_C^* 32.9(-0.45) S_X 15.8(-0.31) K
						K 30.5(0.67) S_X 37.5(0.60) S_C^* 83.4(0.06) S_A 93.4(1.64) I	
3	5	70.1	2.8	1.16	5.5	K 48.9(2.44) S_C^* 89.4(0.06) S_A 103.8(1.70) I	I 96.9(-1.57) S_A 84.7(-0.05) S_C^* 39.9(-0.57) S_X 25.2(-0.31) K
						K 34.0(0.36) S_X 45.4(0.61) S_C^* 89.5(0.05) S_A 104.0(1.62) I	
4	8	75.3	4.3	1.12	8.3	K 52.1(1.98) S_C^* 92.7(0.04) S_A 114.1(1.55) I	I 107.6(-1.52) S_A 88.4(-0.05) S_C^* 47.5(-0.83) S_X
						K 49.2(0.28) S_X 52.8(0.76) S_C^* 93.0(0.04) S_A 114.3(1.53) I	
5	12	74.9	4.9	1.16	9.5	K 59.4(1.88) S_C^* 95.0(0.04) S_A 119.7(1.51) I	I 112.7(-1.48) S_A 90.2(-0.05) S_C^* 52.4(-0.95) S_X
						S_X 59.2(1.21) S_C^* 95.1(0.03) S_A 119.8(1.50) I	
6	20	76.9	6.5	1.13	12.6	K 57.6(0.58) S_X 63.1(1.13) S_C^* 96.6(0.03) S_A 126.4(1.42) I	I 119.6(-1.40) S_A 92.0(-0.05) S_C^* 56.4(-1.01) S_X
						S_X 64.3(1.12) S_C^* 97.9(0.04) S_A 126.5(1.36) I	
7	30	79.7	7.5	1.17	14.6	K 59.0(0.43) S_X 66.3(1.15) S_C^* 97.4(0.03) S_A 128.8(1.37) I	I 122.7(-1.38) S_A 93.8(-0.06) S_C^* 59.8(-1.09) S_X
						S_X 66.4(1.17) S_C^* 97.8(0.04) S_A 129.3(1.36) I	

[a] Polymerization temperature: 0°C; polymerization solvent: methylene chloride; $[M]_o$=0.224; $[Me_2S]_o/[I]_o$=10; polymerization time: 1hour.

[b] Data on first line are from first heating and cooling scans. Data on second line are from second heating scan.

Table III. Characterization of the binary mixtures of monomers **15** with **16**

15/16 (mol)/(mol)	Phase transitions (°C) and corresponding enthalpy changes (kcal/mru)[a]	
	heating	cooling
0/10	K 55.1 (5.97) S_A 60.6 (1.84) I K 54.2 (5.63) S_A 60.5 (1.77) I	I 55.2 (-1.58) S_A 39.6 (-0.05) S_C* 25.9 (-4.01) K
2.1/7.9	K 51.7 (5.49) S_A 61.0 (1.56) I K 50.9 (5.26) S_A 60.9 (1.59) I	I 55.7 (-1.62) S_A 40.0 (-0.02) S_C* 23.9 (-3.67) K
3.8/6.2	K 49.9 (5.43) S_A 61.3 (1.62) I K 48.1 (4.91) S_A 61.2 (1.63) I	I 55.7 (-1.62) S_A 40.0 (-0.03) S_C* 22.3 (-3.44) K
5.1/4.9	K 47.3 (5.14) S_A 61.2 (1.65) I K 45.2 (4.67) S_A 61.1 (1.64) I	I 55.8 (-1.65) S_A 40.1 (-0.03) S_C* 22.3 (-3.38) K
5.9/4.1	K 46.9 (5.07) S_A 61.2 (1.63) I K 44.8 (4.52) S_A 61.2 (1.62) I	I 55.8 (-1.60) S_A 40.7 (-0.04) S_C* 22.7 (-3.31) K
7.8/2.2	K 49.3 (5.08) S_A 61.4 (1.60) I K 48.1 (4.77) S_A 61.3 (1.59) I	I 55.5 (-1.60) S_A 40.9 (-0.05) S_C* 23.8 (-3.47) K
10/0	K 53.3 (5.62) S_A 60.9 (1.82) I K 51.7 (5.17) S_A 60.8 (1.57) I	I 55.4 (-1.57) S_A 41.9 (-0.06) S_C* 26.7 (-3.82) K

[a] Data on first line are from first heating and cooling scans. Data on second line are from second heating scan.

Table IV. Characterization of the binary mixtures of poly(15) with poly(16)

poly(15) DP	poly(16) DP	poly(15)/poly(16) (mol)/(mol)	Phase transitions (°C) and corresponding enthalpy changes (kcal/mru)[a] heating	cooling
6.0	12.6	0/10	K 57.6(0.58) S_X 63.1(1.13) S_C^* 96.6(0.03) S_A 126.4(1.42) I	I 119.6(-1.40) S_A 92.0(-0.05) S_C^* 56.4(-1.01) S_X
			S_X 64.3(1.12) S_C^* 97.9(0.04) S_A 126.5(1.36) I	
6.0	12.6	2/8	K 55.9(1.84) S_C^* 94.3(0.05) S_A 121.6(1.42) I	I 115.2(-1.45) S_A 89.8(-0.06) S_C^* 52.1(-1.13) S_X
			S_X 58.1(1.16) S_C^* 94.0(0.06) S_A 121.2(1.47) I	
6.0	12.6	4/6	K 52.4(2.03) S_C^* 91.6(0.03) S_A 117.3(1.48) I	I 109.7(-1.45) S_A 85.6(-0.04) S_C^* 45.7(-1.20) S_X
			S_X 51.6(1.32) S_C^* 90.2(0.05) S_A 115.9(1.49) I	
6.0	12.6	5/5	K 51.6(1.87) S_C^* 92.6(0.04) S_A 116.1(1.45) I	I 109.2(-1.45) S_A 87.3(-0.05) S_C^* 47.0(-0.97) S_X
			S_X 52.3(1.16) S_C^* 92.0(0.05) S_A 115.5(1.49) I	
6.0	12.6	6/4	K 50.3(2.04) S_C^* 91.0(0.04) S_A 113.4(1.46) I	I 105.0(-1.40) S_A 84.6(-0.03) S_C^* 43.2(-1.05) S_X
			S_X 48.0(1.18) S_C^* 88.4(0.04) S_A 111.7(1.45) I	
6.0	12.6	8/2	K 49.1(2.11) S_C^* 90.5(0.05) S_A 108.9(1.56) I	I 101.7(-1.50) S_A 85.1(-0.04) S_C^* 41.8(-1.05) S_X
			S_X 46.6(1.22) S_C^* 89.5(0.06) S_A 108.2(1.55) I	
6.0	12.6	10/0	K 49.8(2.35) S_C^* 90.9(0.03) S_A 106.5(1.59) I	I 99.6(-1.55) S_A 85.8(-0.06) S_C^* 41.6(-0.52) S_X 30.4(-0.31) K
			K 38.8(0.44) S_X 46.6(0.58) S_C^* 90.4(0.06) S_A 105.9(1.55) I	

[a] Data on first line are from first heating and cooling scans. Data on second line are from second heating scan.

Table V. Cationic Copolymerization of 15 with 16 and Characterization of the Resulting Polymers[a]

Sample No.	[15]/[16] (mol/mol)	Polymer Yield(%)	$Mn \times 10^{-3}$	Mw/Mn	DP	Phase transitions (°C) and corresponding enthalpy changes (kcal/mru)[b]	
						heating	cooling
1	0/10	81.2	6.2	1.10	12.0	K 58.7(0.59) S_X 64.6(1.09) S_C^* 97.0(0.04) S_A 125.4(1.45) I	I 118.8(-1.44) S_A 92.8(-0.06) S_C^* 57.5(-1.07) S_X
						S_X 64.3(1.15) S_C^* 96.7(0.03) S_A 125.0(1.44) I	
2	2/8	80.0	6.0	1.12	11.6	K 57.3(0.58) S_X 63.2(1.09) S_C^* 96.2(0.06) S_A 124.9(1.54) I	I 118.4(-1.44) S_A 91.9(-0.05) S_C^* 56.2(-1.04) S_X
						S_X 63.0(1.19) S_C^* 96.2(0.04) S_A 125.0(1.42) I	
3	4/6	79.9	6.1	1.12	11.9	K 58.5(0.62) S_X 63.3(1.18) S_C^* 96.1(0.04) S_A 125.6(1.47) I	I 119.1(-1.47) S_A 92.0(-0.05) S_C^* 56.6(-1.03) S_X
						S_X 63.2(1.17) S_C^* 96.2(0.04) S_A 125.5(1.47) I	
4	5/5	69.3	6.2	1.10	12.0	K 59.7(0.63) S_X 61.3(1.12) S_C^* 96.0(0.04) S_A 124.9(1.45) I	I 118.6(-1.43) S_A 92.0(-0.06) S_C^* 55.2(-1.05) S_X
						S_X 61.4(1.15) S_C^* 96.1(0.03) S_A 124.9(1.45) I	
5	6/4	82.6	6.5	1.12	12.8	K 59.1(0.64) S_X 64.3(1.14) S_C^* 97.1(0.04) S_A 127.2(1.43) I	I 120.5(-1.43) S_A 92.7(-0.06) S_C^* 58.0(-1.05) S_X
						S_X 63.8(1.20) S_C^* 96.7(0.04) S_A 126.6(1.44) I	
6	8/2	82.4	6.0	1.12	11.7	K 58.9(0.67) S_X 63.9(1.10) S_C^* 97.2(0.04) S_A 126.2(1.44) I	I 119.2(-1.45) S_A 92.5(-0.07) S_C^* 57.3(-1.07) S_X
						S_X 63.7(1.19) S_C^* 97.0(0.03) S_A 126.0(1.44) I	
7	10/0	78.5	6.0	1.13	11.8	K 58.9(0.70) S_X 64.6(1.08) S_C^* 97.8(0.04) S_A 125.8(1.44) I	I 118.7(-1.43) S_A 92.8(-0.06) S_C^* 58.1(-1.00) S_X
						S_X 64.6(1.20) S_C^* 97.9(0.05) S_A 125.8(1.44) I	

[a] Polymerization temperature: 0°C; polymerization solvent: methylene chloride; $[M]_o=[15]+[16]=0.224$; $[M]_o/[I]_o=16$; $[Me_2S]_o/[I]_o=10$; polymerization time: 1hour.

[b] Data on first line are from first heating and cooling scans. Data on second line are from second heating scan.

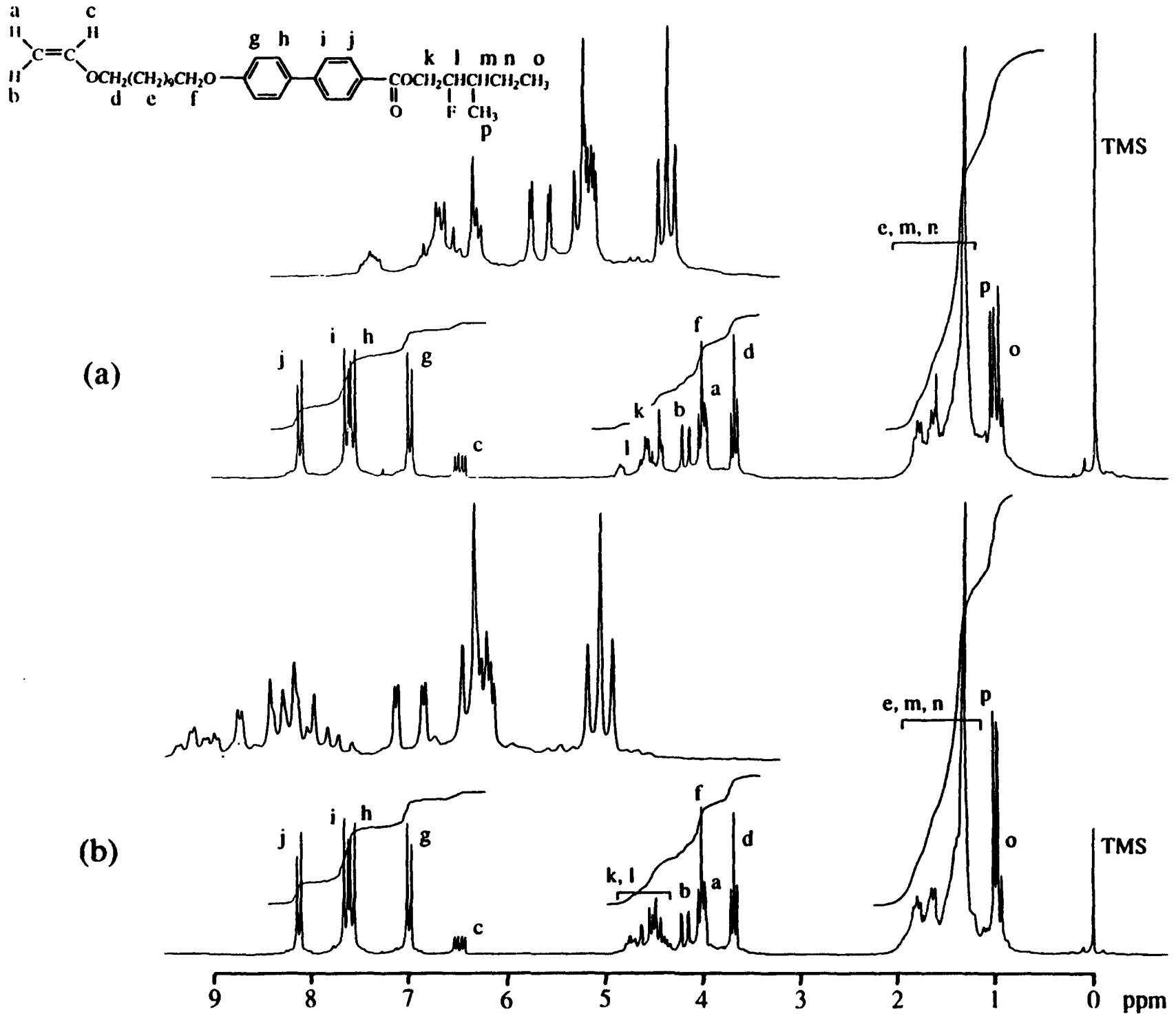
a
c
H
H
C=C
H
H
b
OCH2(CH2)9CH2O
d e f
g h i j
k l m n o
COCH2CHCH2CH2CH3
O
CH3
p
(a)
TMS
e, m, n
p
o
j
i
h
g
c
f
d
a
k
b
l
(b)
TMS
e, m, n
p
o
k, l
9
8
7
6
5
4
3
2
1
0
ppm

Figure 1

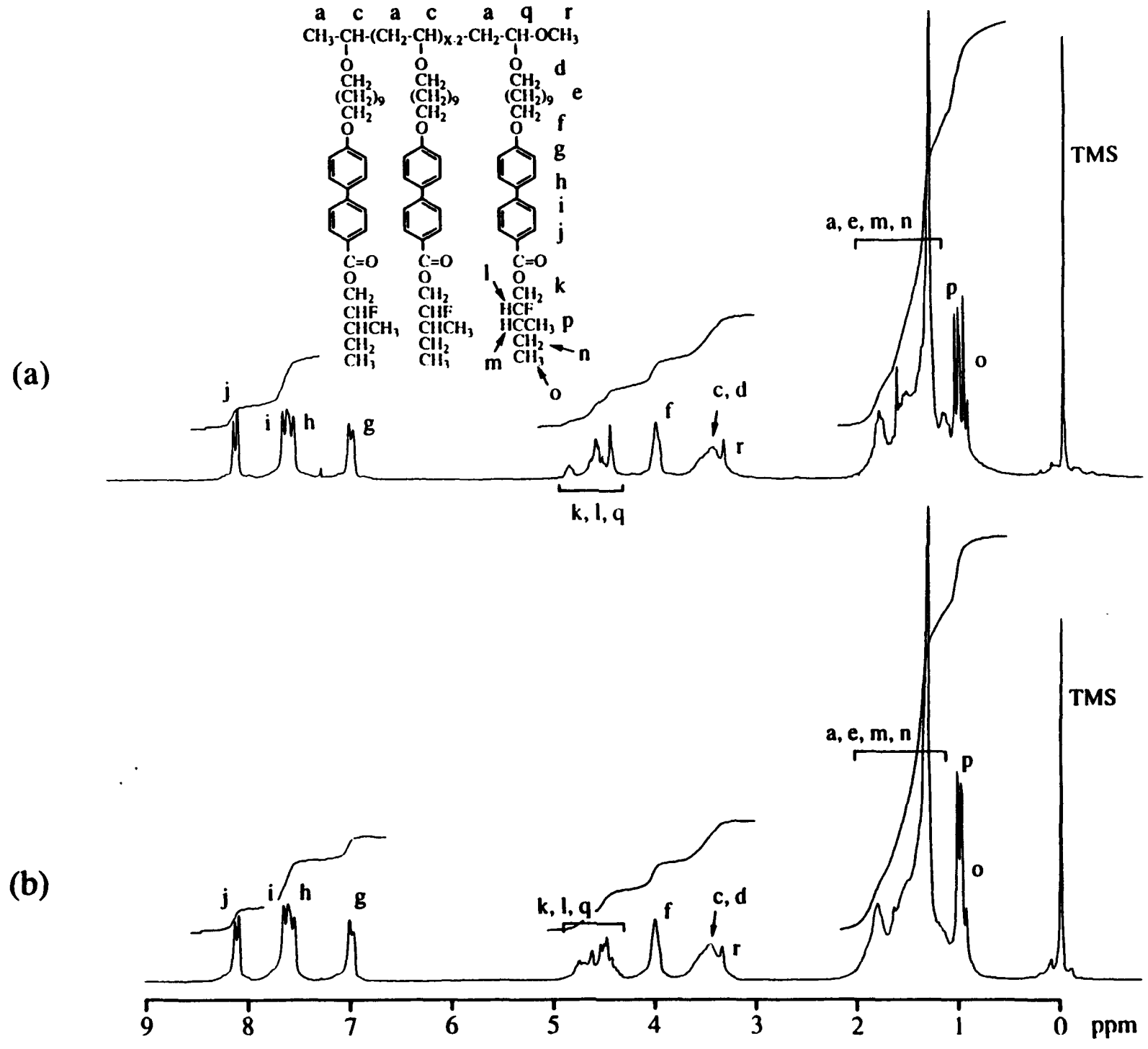

Figure 2

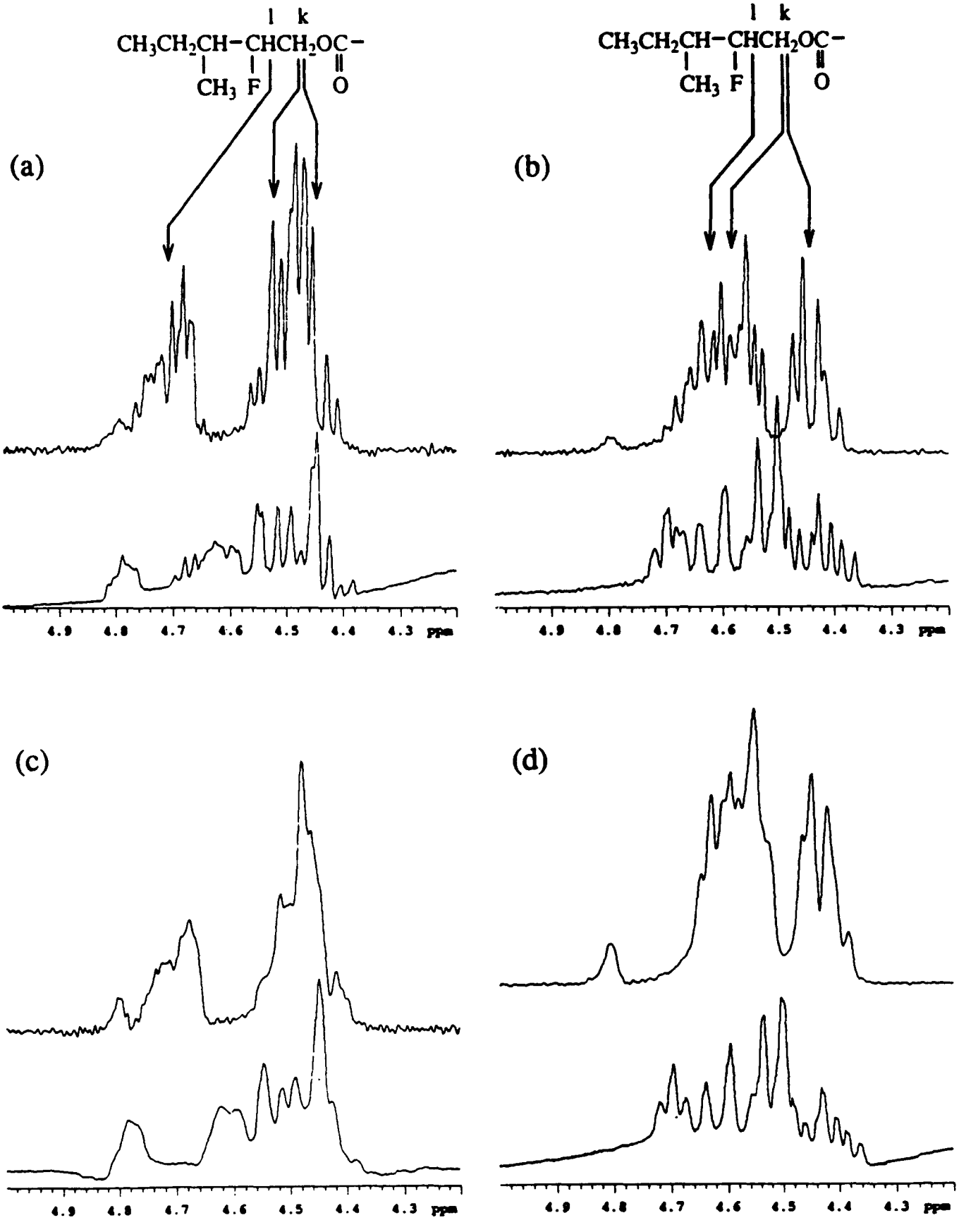

Figure 3

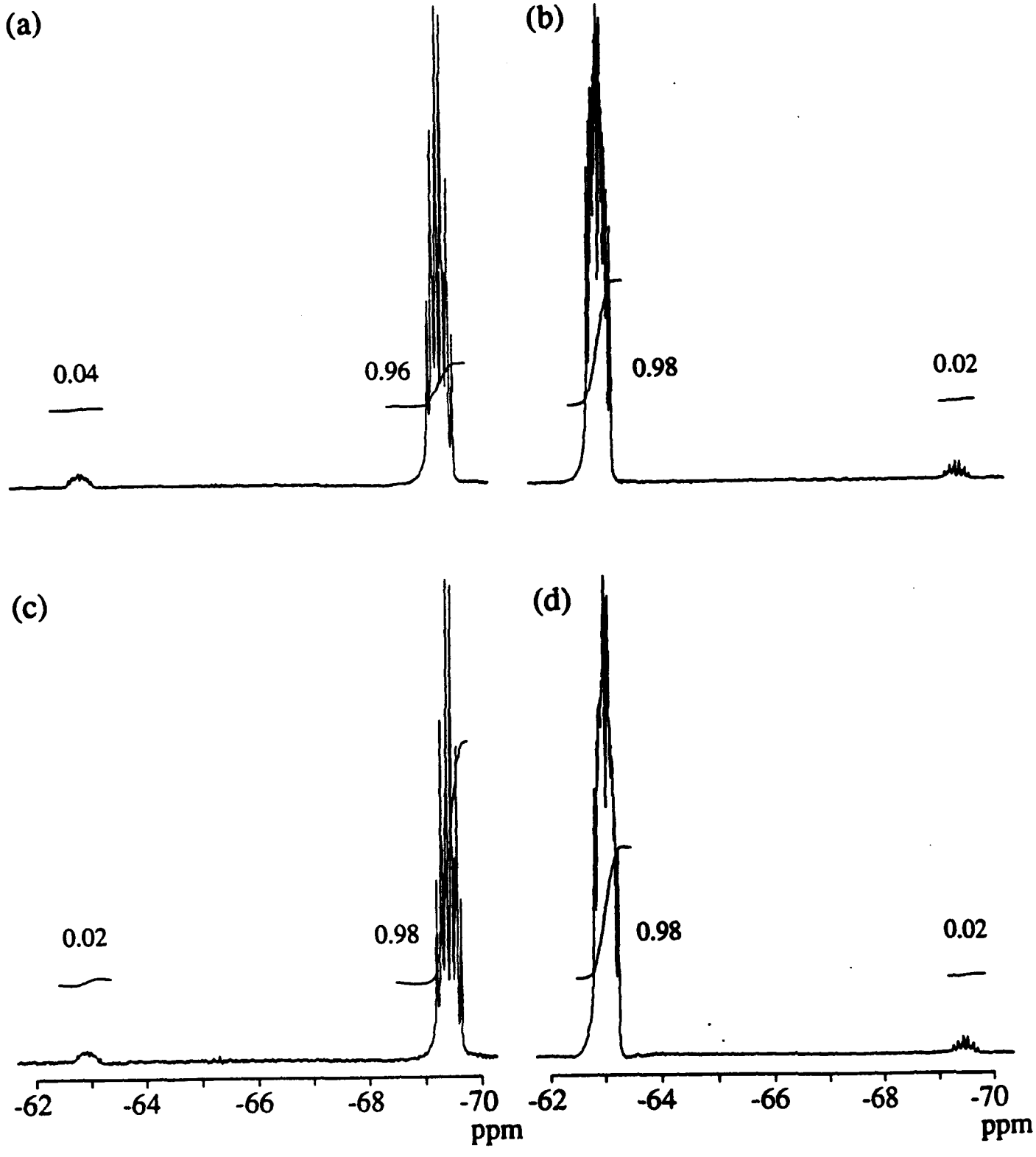
(a)
0.04
0.96
(b)
0.98
0.02
(c)
0.02
0.98
(d)
0.98
0.02
-62
-64
-66
-68
-70
ppm
-62
-64
-66
-68
-70
ppm

Figure 4

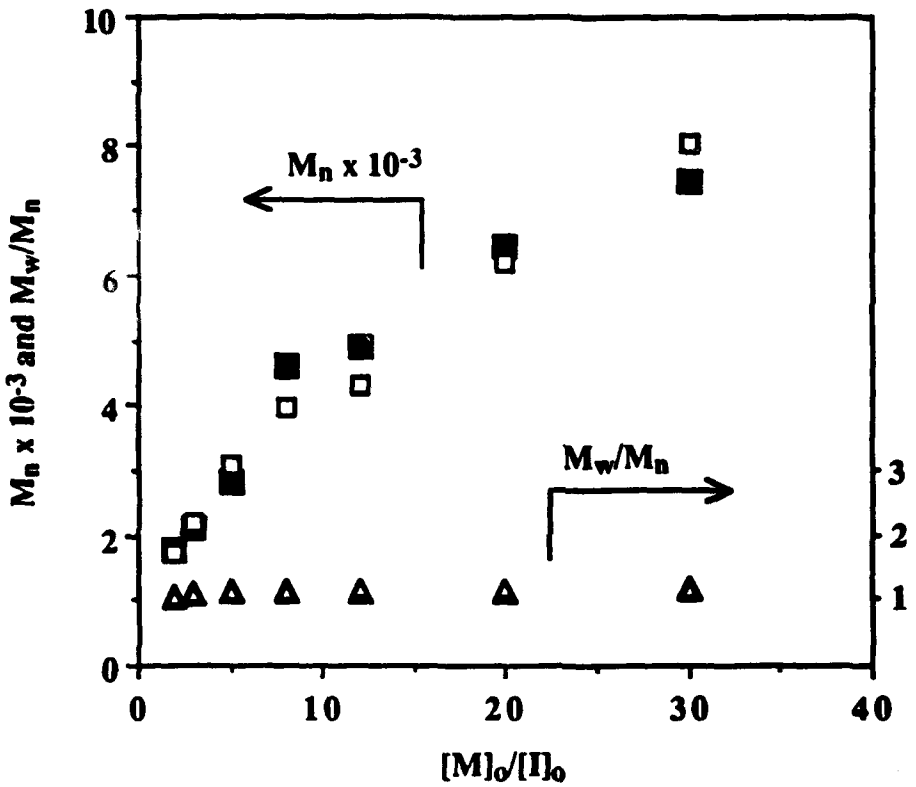

Figure 5

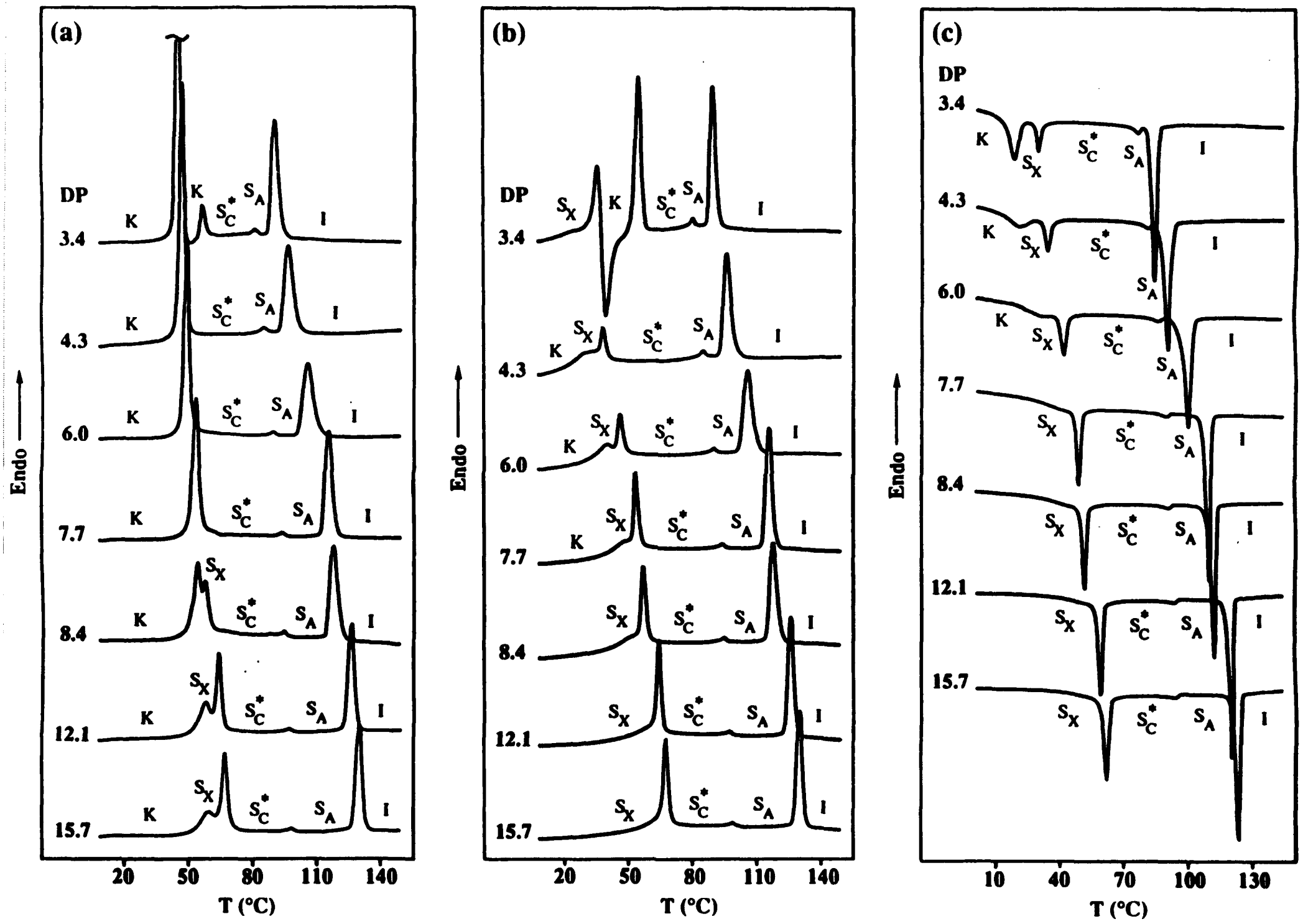
(a)
DP
3.4
4.3
6.0
7.7
8.4
12.1
15.7
K
S_X
S_C^*
S_A
I
Endo
20
50
80
110
140
T (°C)
(b)
DP
3.4
4.3
6.0
7.7
8.4
12.1
15.7
K
S_X
S_C^*
S_A
I
Endo
20
50
80
110
140
T (°C)
(c)
DP
3.4
4.3
6.0
7.7
8.4
12.1
15.7
K
S_X
S_C^*
S_A
I
Endo
10
40
70
100
130
T (°C)

Figure 6

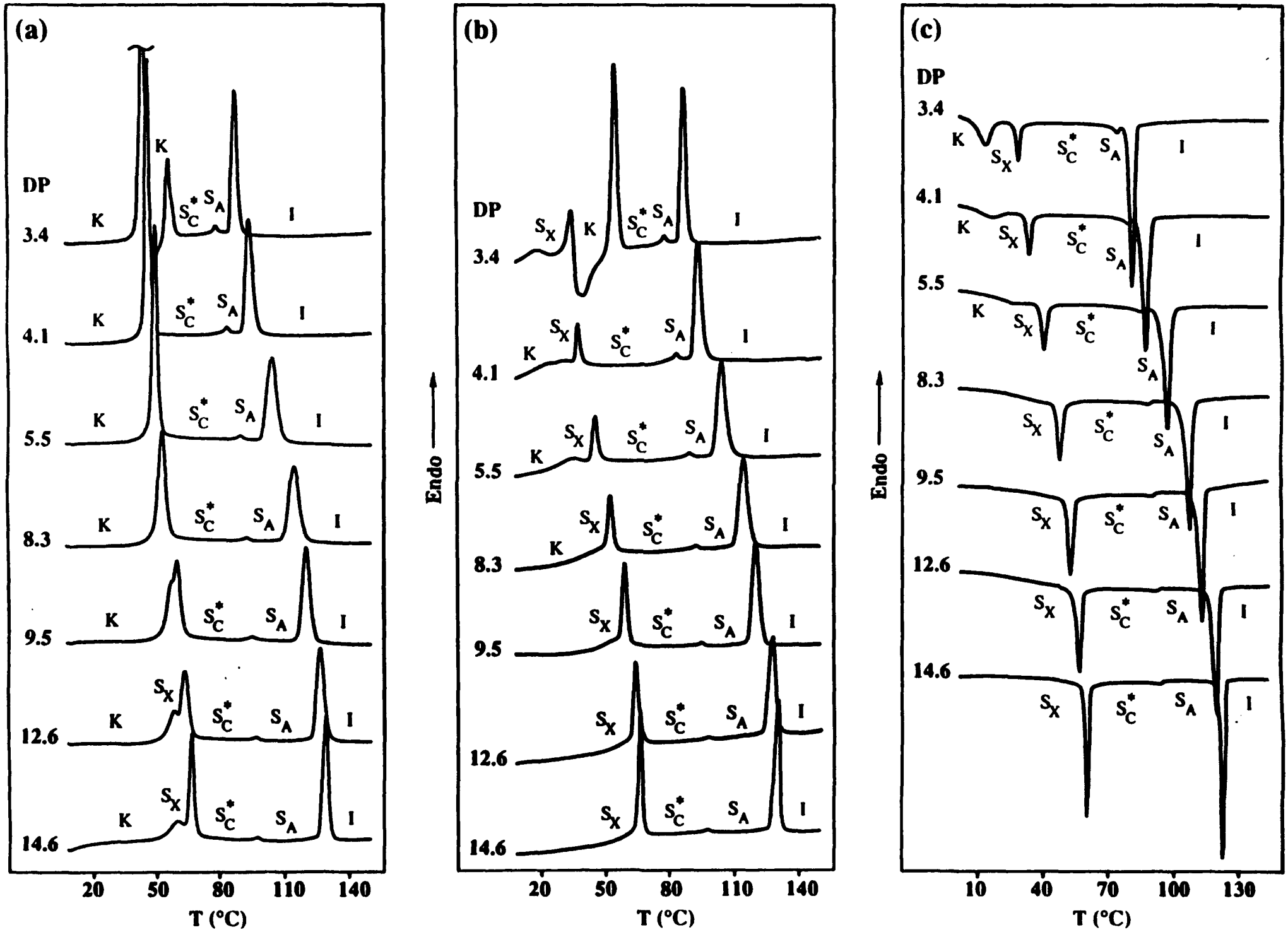
(a)
DP
3.4
4.1
5.5
8.3
9.5
12.6
14.6
K
S_X
S_C^*
S_A
I
Endo
20
50
80
110
140
T (°C)
(b)
DP
3.4
4.1
5.5
8.3
9.5
12.6
14.6
K
S_X
S_C^*
S_A
I
Endo
20
50
80
110
140
T (°C)
(c)
DP
3.4
4.1
5.5
8.3
9.5
12.6
14.6
K
S_X
S_C^*
S_A
I
Endo
10
40
70
100
130
T (°C)

Figure 7

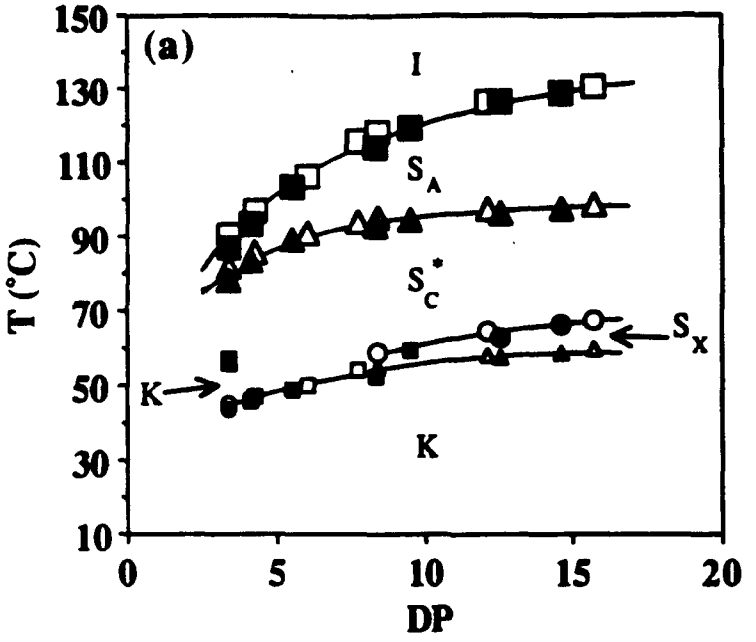
(a)
I
S_A
S_C^*
S_X
K
K
T (°C)
DP
150
130
110
90
70
50
30
10
0
5
10
15
20

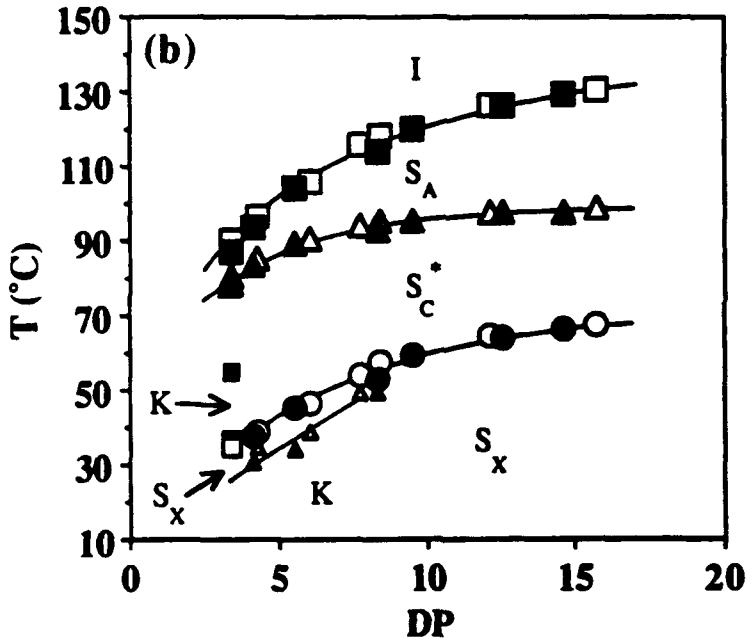
(b)
I
S_A
S_C^*
K
S_X
S_X
K
T (°C)
DP
150
130
110
90
70
50
30
10
0
5
10
15
20

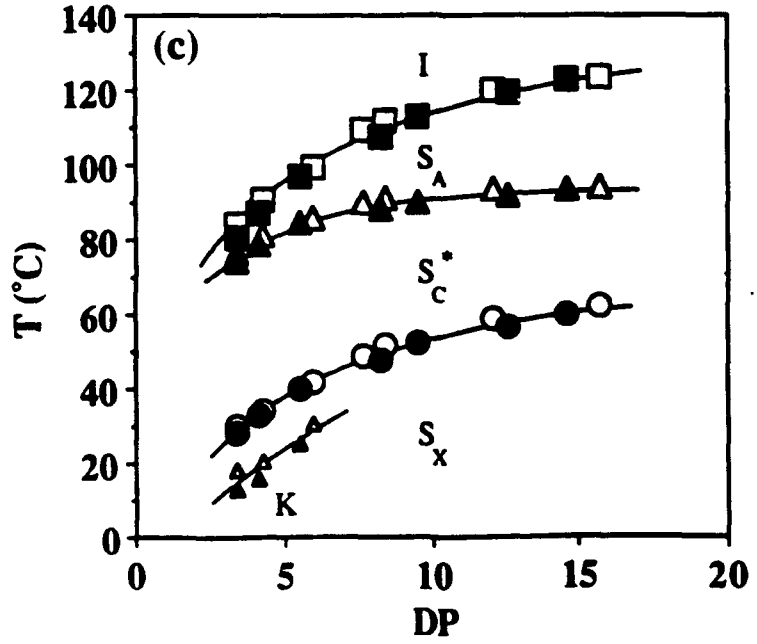
(c)
I
S_A
S_C^*
S_X
K
T (°C)
DP
140
120
100
80
60
40
20
0
0
5
10
15
20

Figure 8

(a)

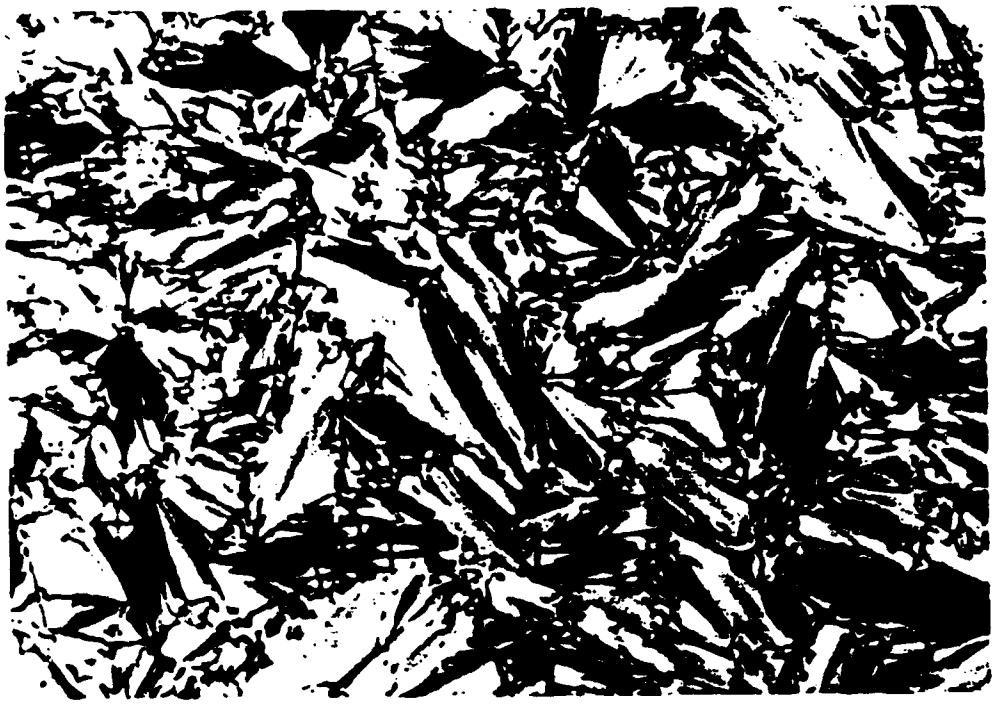

(b)

Figure 9

(c)

(d)

Figure 9

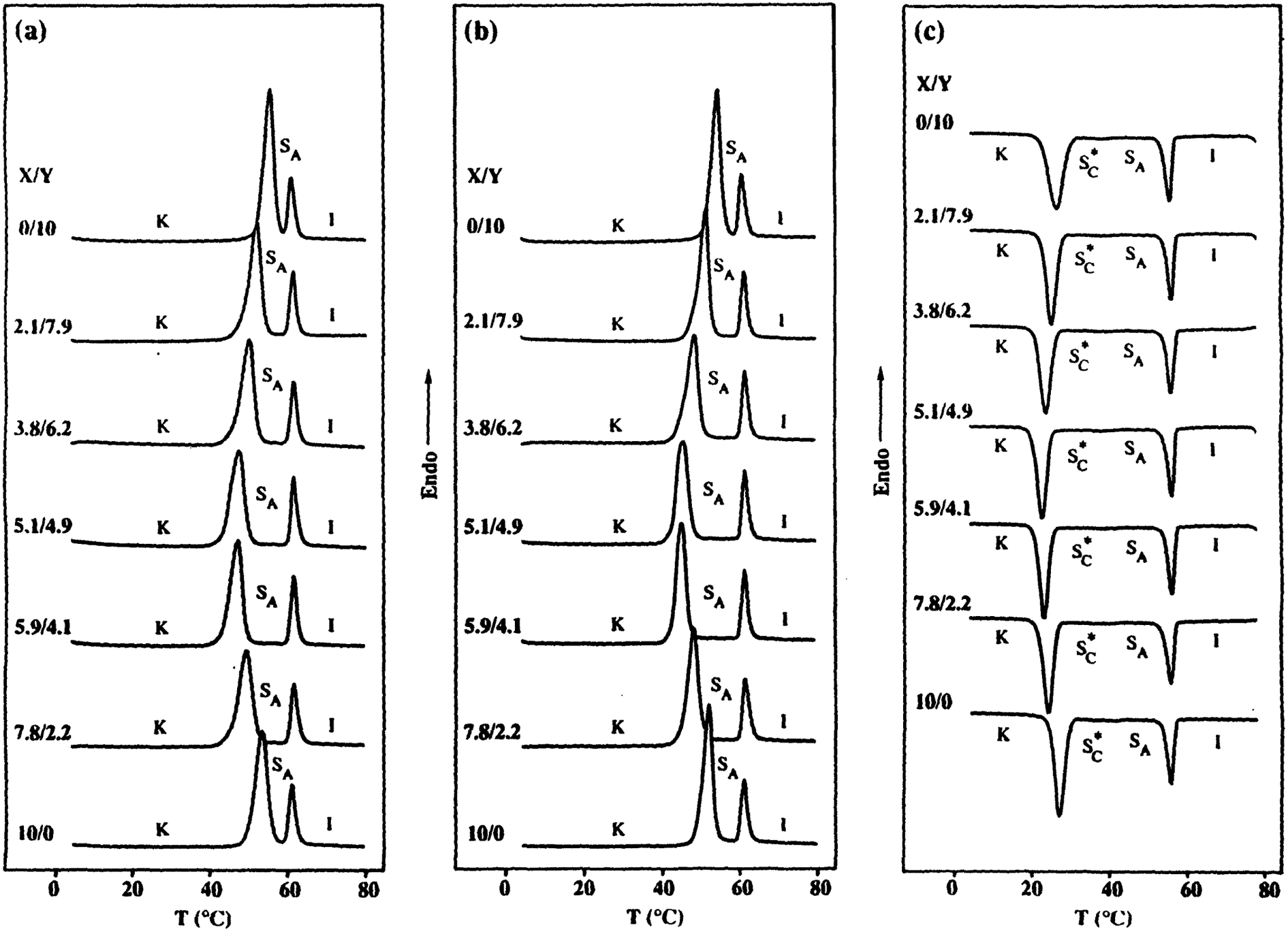
(a)
X/Y
0/10
2.1/7.9
3.8/6.2
5.1/4.9
5.9/4.1
7.8/2.2
10/0
K
S_A
I
0
20
40
60
80
T (°C)
(b)
Endo
(c)
S_C^*

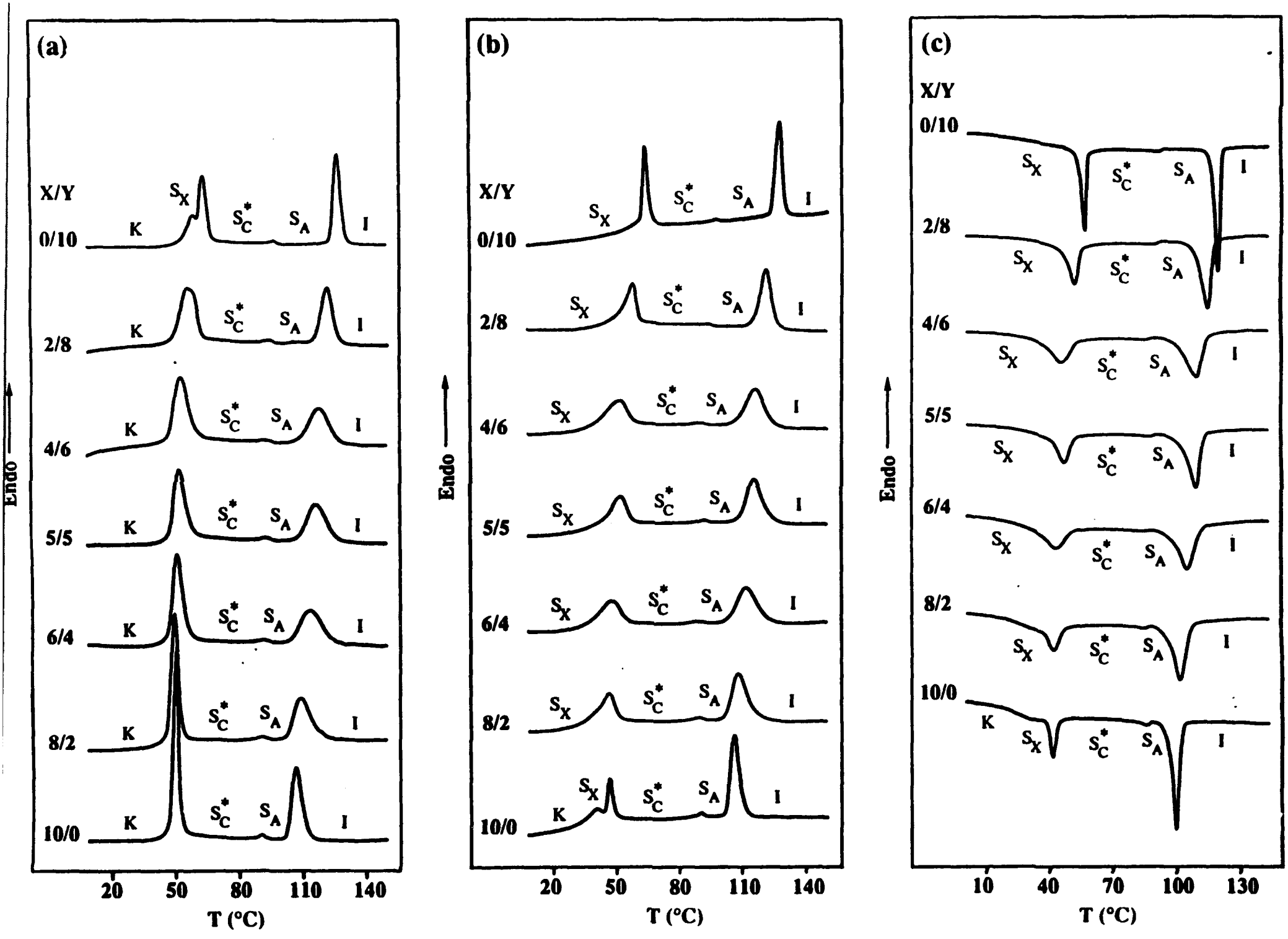
(a)
X/Y
0/10
2/8
4/6
5/5
6/4
8/2
10/0
K
S_X
S_C^*
S_A
I
Endo
20
50
80
110
140
T (°C)
(b)
X/Y
0/10
2/8
4/6
5/5
6/4
8/2
10/0
K
S_X
S_C^*
S_A
I
Endo
20
50
80
110
140
T (°C)
(c)
X/Y
0/10
2/8
4/6
5/5
6/4
8/2
10/0
K
S_X
S_C^*
S_A
I
Endo
10
40
70
100
130
T (°C)

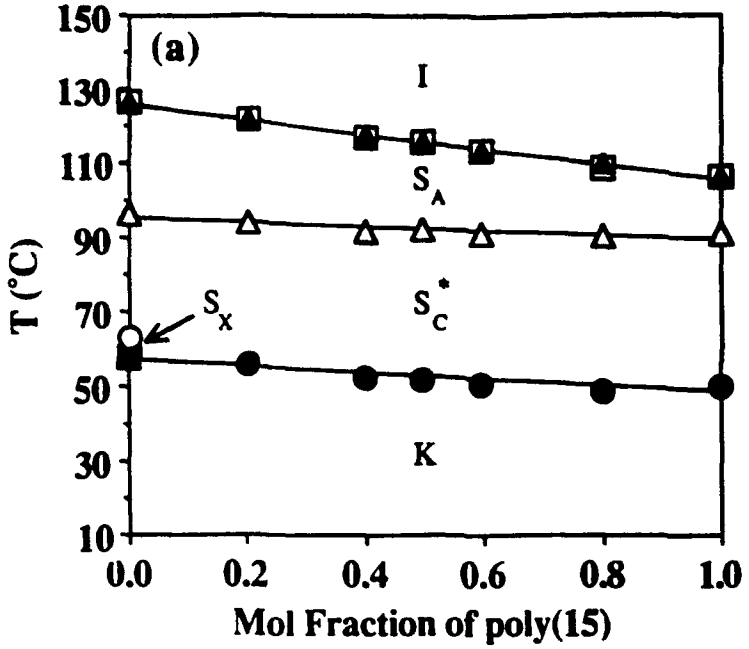
(a)
I
S_A
S_C^*
S_X
K
T (°C)
150
130
110
90
70
50
30
10
0.0
0.2
0.4
0.6
0.8
1.0
Mol Fraction of poly(15)

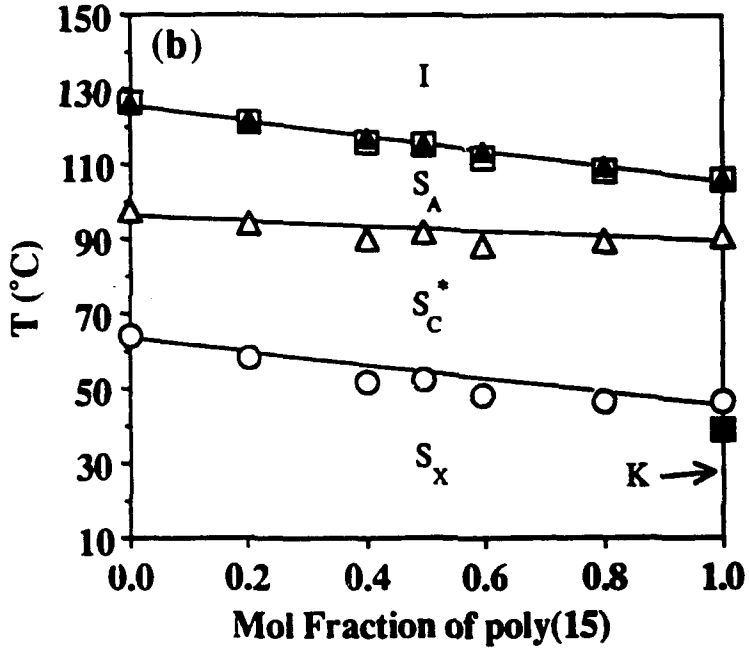
(b)
I
S_A
S_C^*
S_X
K
T (°C)
150
130
110
90
70
50
30
10
0.0
0.2
0.4
0.6
0.8
1.0
Mol Fraction of poly(15)

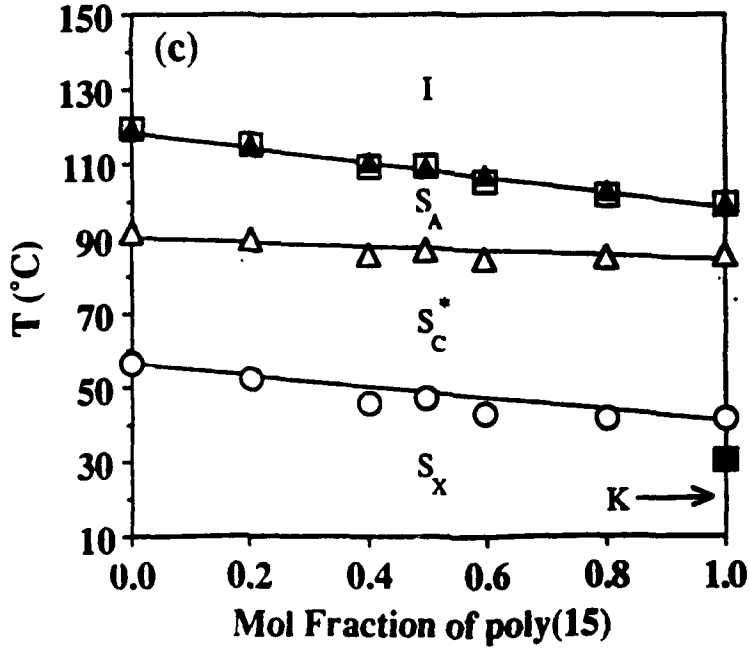
(c)
I
S_A
S_C^*
S_X
K
T (°C)
150
130
110
90
70
50
30
10
0.0
0.2
0.4
0.6
0.8
1.0
Mol Fraction of poly(15)

Figure 13

Figure 14

Figure 18

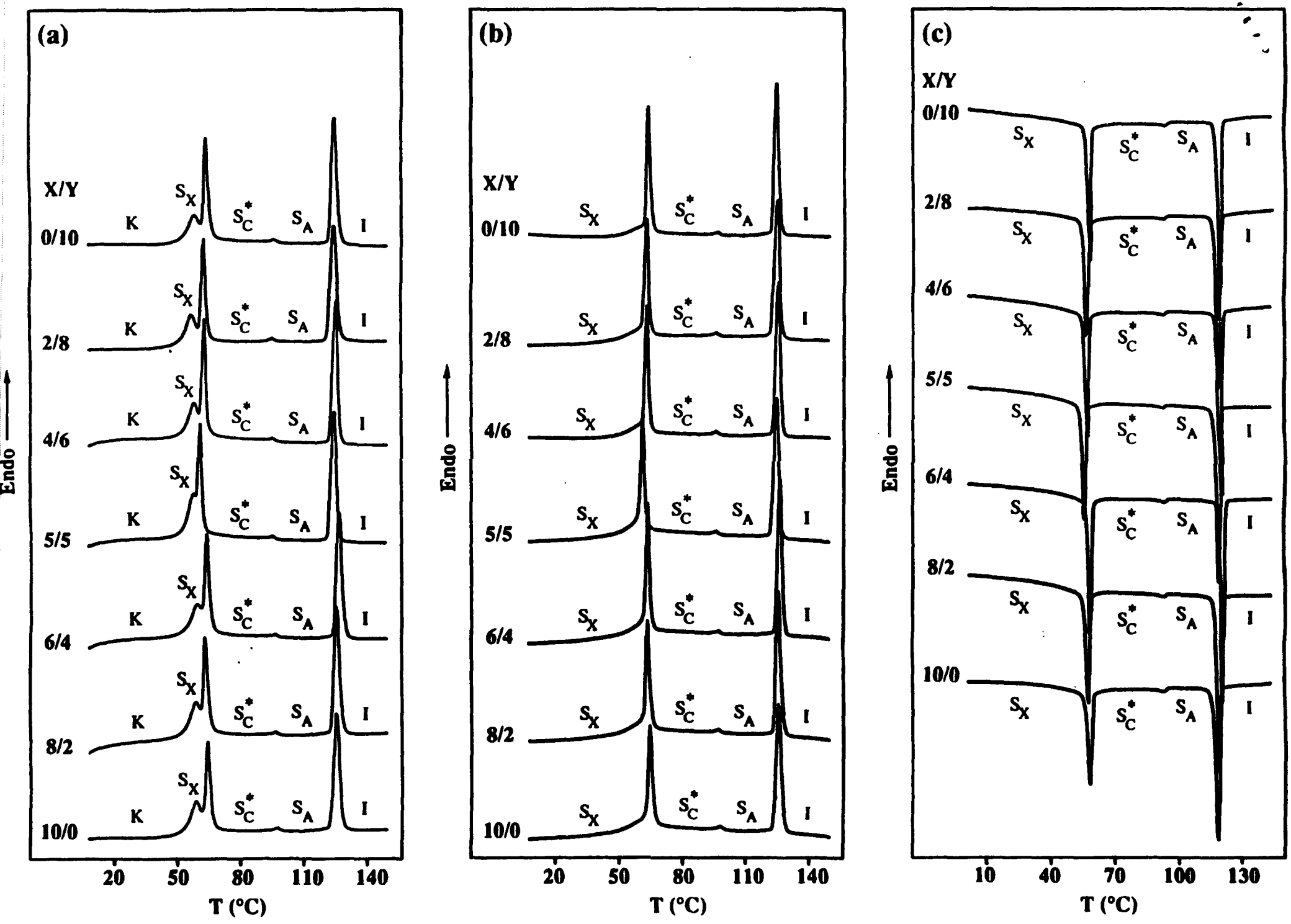
(a)
X/Y
0/10
2/8
4/6
5/5
6/4
8/2
10/0
K
S_X
S_C^*
S_A
I
Endo
20
50
80
110
140
T (°C)
(b)
X/Y
0/10
2/8
4/6
5/5
6/4
8/2
10/0
S_X
S_C^*
S_A
I
Endo
20
50
80
110
140
T (°C)
(c)
X/Y
0/10
2/8
4/6
5/5
6/4
8/2
10/0
S_X
S_C^*
S_A
I
Endo
10
40
70
100
130
T (°C)

Figure 15